DOI: 10.5281/zenodo.15076433

CURRENT APPROACHES IN MECHANICAL ENGINEERING

EDITOR
Prof. Hasan Öktem, Ph.D.

Current Approaches in Mechanical Engineering

EDITOR

Prof. Hasan Öktem, Ph.D.

Publisher
Platanus Publishing®

Editor in Chief
Prof. Hasan Öktem, Ph.D.

Cover & Interior Design
Platanus Publishing®

Editorial Coordinator
Arzu Betül Çuhacıoğlu

The First Edition
March, 2025

Publisher's Certificate No
45813

ISBN

978-625-6634-97-8

Platanus Publishing®
Address: Natoyolu Cad. Fahri Korutürk Mah. 157/B, 06480, Mamak, Ankara, Turkey.
Phone: +90 312 390 1 118
web: www.platanuskitap.com
e-mail: platanuskitap@gmail.com

PLATANUS PUBLISHING®

CONTENTS

CHAPTER 1

Digital Carbon Footprint and Sustainable Solutions

Gamze Yakut[1]

[1] Assist. Prof. Isparta Uygulamalı Bilimler Üniversitesi, OSB Meslek Yüksekokulu Mekatronik Programı
ORCID: 0000-0002-8614-304X

1. ENVIRONMENTAL STATUS OF DIGITALIZATION

The recent acceleration of technological innovation has led to paradigm shifts in socioeconomic systems, while its impacts on natural resource consumption and the climate system are increasingly becoming the focus of scientific research. Studies reveal that the environmental impacts arising throughout the life cycle (raw material extraction, production, use, waste management) of digital technologies and related infrastructure are multi-layered and complex. In particular, the extraction and processing of rare earth elements and other critical minerals used in the production of electronic devices have been shown to have impacts on ecosystem degradation, biodiversity loss, and water resources (Kim et. al., 2021; Watari et. al., 2019). Furthermore, the increasing energy demand of data centers and communication networks, largely dependent on fossil fuel-based electricity generation, is highlighted as a significant source of greenhouse gas emissions and contributes to global climate change (Jones, 2018; Shehabi et. al., 2016). Electronic waste (e-waste), resulting from rapid technological obsolescence and consumption trends, poses serious risks to both human health and the environment due to its toxic substance content and inadequate recycling practices (Akenji et. al., 2021; Baldé et. al., 2017). In this context, the need to manage technological developments in line with environmental sustainability principles, adopt circular economic approaches, and integrate life cycle assessments (LCA) into decision-making processes comes to the fore.

The digital carbon footprint is a concept that refers to the entirety of environmental impacts caused by digital technologies and online activities throughout their entire life cycle, especially greenhouse gas (GHG) emissions and energy consumption (Cahyaningrum et. al., 2025; Ericsson, 2025; Nutanix, 2025; Riabova, 2025). This impact is not limited to the use of individual devices (smartphones, computers, tablets, etc.), but also includes processes such as the production of these devices, the operation of internet infrastructure (data centers, network equipment, base stations), the provision of digital services (cloud computing, video streaming, social media, e-mail, etc.), and the storage and processing of digital data (Kang et. al., 2025; T. A. Et. al., 2025). The digital carbon footprint also includes other environmental impacts such as water use, electronic waste (e-waste) generation, and depletion of natural resources.

The contribution of information and communication technologies (ICT) to global greenhouse gas emissions is a growing concern. According to The Shift Project's (2018) report, the ICT sector is responsible for approximately 4% of global emissions. This rate is projected to rise to 14% by 2040 with the acceleration of technological developments and digitalization (The Shift Project, 2018). Even at the individual level, the environmental impact of digital activities cannot be ignored. For example, according to calculations by Berners-Lee (2020), an average e-mail causes approximately 4 grams of CO2e (carbon dioxide equivalent) emissions. These data clearly demonstrate the need for urgent and comprehensive measures to reduce the environmental impact of the ICT sector.

The environmental impact of information and communication technologies (ICT), particularly its contribution to global greenhouse gas emissions, has received increasing attention in academic and political circles in recent years. According to The Shift Project (2020) data, the ICT sector is currently responsible for approximately 4% of global emissions, and this rate is projected to rise to 14% by 2040 (Gandhi et. al., 2023). These projections are associated with the rapid growth of the digital economy and increasing demands for data processing, storage, and transmission. The environmental impacts of individual digital activities should not be overlooked; it is estimated that an average e-mail causes approximately 4 grams of CO2e (carbon dioxide equivalent) emissions (Naeem et. al., 2023). These seemingly small emissions, considering that billions of e-mails are sent globally, contribute significantly to the total carbon footprint of ICT. In this context, policymakers, businesses, and individuals need to develop and implement strategies to reduce the environmental impacts of digital activities. Promoting energy-efficient technologies, data center optimization, and adopting sustainable digital practices are among the key elements of these strategies.

2. SOURCES OF DIGITAL CARBON FOOTPRINT

Device Production

The production of digital devices, ranging from smartphones to laptops, tablets to servers, is a complex and multi-stage process. This process begins with the extraction of rare earth elements, precious metals (such as gold, palladium, and silver), and petroleum-derived plastics from the depths of the earth's crust (Widmer et. al., 2005; Williams, 2011). The extraction and processing of these raw materials are processes that are both energy-intensive and environmentally destructive due to the nature of mining activities (Kim et. al., 2021). For example, opening mines can lead to soil erosion, contamination of water resources, and loss of biodiversity. During the processing of raw materials, high temperatures, chemical reactions, and refining processes cause significant energy consumption and greenhouse gas emissions. At the production stage, assembly lines in factories, testing processes, and other production activities increase electricity consumption and lead to additional emissions using various chemicals (e.g., clean solvents, soldering materials) (O'Connell and Stutz, 2010). The designs and marketing strategies of manufactured devices often encourage them to be short-lived and consumers to constantly purchase new models. This situation brings with it a rapidly growing e-waste problem. Electronic waste (e-waste) poses serious risks to both the environment and human health due to the hazardous substances it contains (such as mercury, lead, and cadmium) and inadequate recycling infrastructure (Akenji et. al., 2021; Baldé et. al., 2017; Forti et. al., 2020). The inadequacy of recycling processes prevents the recovery of valuable metals and other resources, while also causing toxic substances to be released into the soil, water, and air. This negative picture clearly shows how important it is to transition to more sustainable production and consumption models in accordance with circular economy principles to reduce the environmental impacts of digital technologies (Geissdoerfer et. al., 2017). These new models aim to promote longer product lifespans, repairability, reusability, and recyclability.

Data Centers

Data centers are critical infrastructure elements that form the backbone of information and communication technologies (ICT) and can be described as the heart of the modern digital economy. However, these centers consume large amounts of energy and create a significant carbon footprint as they perform intensive operations such as routing internet traffic, storing, processing, and presenting data. In fact, global data center electricity use in 2020 was estimated to be between 200-250 TWh; this amount corresponds to approximately 1% of the global final electricity demand for that year and is even higher than the total electricity consumption of some countries (Masanet et. al., 2020). Some projections even predict that data center electricity consumption could reach 8% of global electricity demand by 2030 (Andrae, 2020). A significant portion of this energy is used by the advanced cooling systems needed to keep the thousands, or even tens of thousands, of servers and other IT equipment in data centers at optimum operating temperature (usually between 18-27°C) (Shehabi et. al., 2016). Traditional cooling systems typically use high-energy consuming compressor-based air conditioners and cooling towers. Some refrigerants used in these systems (e.g., hydrofluorocarbons - HFCs) are thousands of times more potent greenhouse gases than carbon dioxide (CO2) and have a much greater impact on global warming when released into the atmosphere (R1234yf, 2024; Zilio et. al., 2011). The rapid proliferation of cloud computing and big data applications is exponentially increasing the demand for data centers and making this impact even more pronounced (Andrae & Edler, 2015; Salahuddin & Alam, 2016). This situation makes solutions such as increasing the energy efficiency of data centers, accelerating the transition to renewable energy sources (solar, wind, geothermal, etc.), developing and using more efficient cooling technologies (e.g., liquid cooling, free cooling), recovering waste heat, and even locating data centers in climatically more suitable regions critically important in reducing the digital carbon footprint.

Network Infrastructure

Internet traffic, as an indispensable element of modern digital life, refers to a continuous and exponentially increasing flow of data on a global scale. In order to ensure this massive data flows uninterruptedly and reliably, a globally widespread and heterogeneous network infrastructure is required, which is operational 24/7, performing complex and energy-intensive operations such as transmitting, routing, processing, and storing data around the world. This infrastructure extends from intercontinental submarine fiber optic cables (which carry more than 99% of global internet traffic) to terrestrial fiber optic networks, cellular networks (3G, 4G, 5G, and beyond), Wi-Fi networks, routers, switches, base stations, satellite communication systems, content delivery networks (CDNs), and many other network hardware and software components. Each component of this system requires different amounts of electrical energy to operate; however, the total energy consumption of these components reaches a very large amount when considered on a global scale.

Mobile networks and the base stations that form the basis of these networks are energy-intensive units due to the nature of cellular communication (continuous signal transmission and reception, connecting with mobile devices, data encryption, etc.) (Agiwal et. al., 2023; Nayeri et. al., 2021). The annual energy consumption of a base station can vary depending on the region, the technology used, traffic density, and other factors, but it can typically be between a few thousand kWh and tens of thousands of kWh. Considering that there are millions of base stations around the world and this number is constantly increasing, the magnitude of the total energy consumption and carbon footprint of mobile networks can be better understood. The proliferation of 5G technology offers significant advantages such as higher data rates, lower latency, and the ability to support more devices, but it also brings new challenges in terms of energy consumption. 5G requires a larger number and more densely deployed base stations (especially small cells) compared to previous generation mobile networks, and because it uses higher frequency bands, signal propagation is more limited (Fettweis & Alamouti, 2014; Gupta & Jha, 2015; Andrews et. al., 2014).

This situation can potentially increase the energy consumption and carbon footprint of 5G networks (Williams et. al., 2022; Li et. al., 2021).

In addition, the explosion in the number of Internet of Things (IoT) devices (more than 50 billion IoT devices are expected to be connected to the internet by 2030) and the impact of artificial intelligence (AI) applications on network traffic are other important factors that increase the energy consumption of the network infrastructure (Borgia et. al., 2016; Ge et. al., 2018). Therefore, a multifaceted and holistic approach is needed to improve the energy efficiency of network infrastructure. This approach should include developing and using less energy-consuming chips, base stations, and other network equipment on the hardware side; developing algorithms and protocols that optimize network traffic on the software side (e.g., sleep modes, traffic routing, content caching); using renewable energy sources (solar, wind) in base stations and other network facilities on the infrastructure side, developing and implementing green network technologies (e.g., energy harvesting, smart grids); and strategies such as network planning and optimization, energy management systems, and data center integration on the operational side.

User Behaviors

The daily digital habits and preferences of individual users, although seemingly insignificant at first glance, contribute surprisingly large and increasingly to the digital carbon footprint when considered on a global scale where billions of users exhibit similar behaviors. This contribution is influenced by a wide variety of factors, from the type of devices we use, the time we spend on the internet, the websites we visit, the applications we use, the videos we watch, to the emails we send.

In particular, video streaming services (Netflix, YouTube, Amazon Prime Video, Disney+, etc.), due to their central role in the modern understanding of entertainment and the increasing preference for high-definition (HD, 4K, 8K) content, constitute a significant component of the digital carbon footprint. A high-definition video requires much more data transfer than a standard-definition video, which leads to more energy consumption both on the user's device (smartphone, tablet, computer, smart TV) and in data centers and network infrastructure (Coroama & Hilty, 2014; Afzal et. al., 2019; Freitag et. al., 2021). For example, according to Netflix's own data, one hour of HD video streaming consumes approximately 1 GB of data, while 4K video streaming can consume up to 7 GB of data. This data transfer means electricity consumption that leads to CO_2 emissions.

Although e-mails are an indispensable tool of modern communication, unnecessary e-mails (spam, promotional e-mails, unread newsletters), e-mails with large attachments, and long e-mail chains are stored and transmitted both on the sender's and recipient's devices and on e-mail servers (data centers); this causes energy consumption and therefore carbon emissions (Berners-Lee, 2020; Pihkola et. al., 2010). The carbon footprint of an e-mail varies depending on its size, attachments, and the number of recipients; however, it is estimated that an average e-mail causes approximately 4 grams of CO2e (carbon dioxide equivalent) emissions.

Social media platforms (Facebook, Instagram, Twitter, TikTok, etc.) are platforms where users are constantly exposed to content streams, watch automatically played videos, share photos and videos, comment, and like, in short, are in intense interaction. This constant interaction causes users' devices to consume more energy (especially shortening battery life) and thus increases the carbon footprint (Batmunkh, 2022; Freitag et. al., 2021).

Online games, especially games that require high graphics, multiplayer, and real-time interaction (Fortnite, Call of Duty, League of Legends, etc.), cause high energy consumption both on the user's device (game console, computer) and on game servers (data centers). These games often require powerful graphics processing units (GPUs), which consume a significant amount of electricity (Weber et. al., 2010; Mills et. al., 2019).

Cryptocurrency mining, especially cryptocurrencies that use the Proof-of-Work (PoW) consensus algorithm such as Bitcoin, Ethereum (during the Proof-of-Work period), requires special hardware (ASIC miners) designed to solve complex mathematical problems to add new blocks to the blockchain and verify transactions. This hardware consume very high amounts of electrical energy, which causes a significant carbon footprint and environmental impacts (de Vries, 2018; Köhler & Pizzol, 2019; Stoll et. al., 2019; Gallersdörfer et. al., 2020). The annual energy consumption of Bitcoin mining is estimated to be higher than the total electricity consumption of some countries.

In conclusion, reviewing our individual digital habits, making more conscious and sustainable choices (e.g., lowering video resolution, avoiding unnecessary e-mails, limiting the time we spend on social media, using less energy-consuming devices, turning to more environmentally friendly alternatives instead of cryptocurrency mining) are important steps we can take to reduce our digital carbon footprint and contribute to a more sustainable digital future.

3. METHODS AND CHALLENGES OF MEASURING DIGITAL CARBON FOOTPRINT

Life Cycle Assessment (LCA)

Life Cycle Assessment (LCA) is a systematic and quantitative methodology based on internationally accepted standards (ISO 14040 and ISO 14044) that comprehensively evaluates the environmental impacts of a product, process, or service with a "cradle-to-grave" or increasingly "cradle-to-cradle" approach, i.e., from the extraction of raw materials to the production, transportation, use, end-of-life disposal or recycling/reuse stages (ISO, 2006a; ISO, 2006b; Curran, 2006). LCA evaluates not only the carbon footprint (greenhouse gas emissions) but also a number of different environmental impact categories such as water footprint, land use, eutrophication, acidification, ozone depletion, human health impacts, ecotoxicity, resource depletion (minerals, fossil fuels, etc.) (Rebitzer et. al., 2004; Guinée et. al., 2002).

In the context of digital technologies, LCA is a critical tool for quantitatively determining the environmental impacts of digital devices such as smartphones, laptops, tablets, servers, data storage devices, network equipment (routers, switches, base stations, etc.) and digital infrastructures such as data centers, cloud computing services, and telecommunication networks. LCA analyzes a wide range of environmental impacts, from the environmental impacts of the extraction and processing of rare earth elements (neodymium, dysprosium, praseodymium, etc.) used in the production of a smartphone (habitat destruction, water pollution, toxic waste caused by mining activities) to the source of energy used during the assembly of the device and the emissions during the production of this energy, to the source of electrical energy consumed by the device during its lifetime (coal, natural gas, nuclear, renewable energy) and the greenhouse gas emissions during the production of this energy, to the challenges of managing the device as electronic waste (e-waste) at the end of its life (release of toxic substances into the environment, recovery of valuable metals) (Van Geet & Sickinger, 2024; Belkhir & Elmeligi, 2018; Itten et. al., 2020; Cordella et. al., 2021).

LCA studies are critical for developing strategies to reduce the environmental impacts of digital technologies, making more sustainable product designs (e.g., using less energy-consuming components, making modular designs, using recycled materials), implementing circular economy principles (extending product life, promoting repair and reuse, facilitating recycling), improving supply chain management, and informing policymakers and consumers. For example, if an LCA study shows that more than 80% of the carbon footprint of a smartphone comes from the production phase, this indicates that manufacturers should focus on improving their production processes and using more sustainable materials.

However, LCA also has some limitations. LCA is a data-intensive process and requires a large amount of high-quality data to obtain accurate and reliable results. Collecting this data can be difficult and time-consuming, especially for digital products with complex supply chains. In addition, the assumptions and modeling options used in LCA can significantly affect the results. Therefore, LCA studies should be reported transparently, and the results should be interpreted carefully.

Carbon Footprint Calculators

Carbon footprint calculators are user-friendly tools, usually accessible online, that help individuals, households, organizations, products, services, or specific activities (e.g., a plane trip, a car trip, a building's energy consumption, a website's hosting, an email sent) estimate their greenhouse gas emissions (usually in carbon dioxide equivalent - CO2e). These calculators ask users to enter various data such as energy consumption (electricity, natural gas, fuel), transportation habits (car use, plane trips, public transportation), dietary preferences (meat consumption, local products, organic foods), waste generation (recycling, composting), lifestyle choices (house size, shopping habits). Based on this data, the calculators provide a carbon footprint estimate, usually using standardized emission factors (the amount of greenhouse gas emissions per unit of activity) published by national or international organizations (e.g., IPCC, EPA) (Carbonfootprint.com, 2025; EPA, 2024; Accounting, 2004).

Specifically for the digital carbon footprint, some calculators focus on estimating the carbon footprint of digital activities such as internet use (web browsing, video streaming, online games), device use (smartphone, computer, tablet), data storage (cloud services, local storage), sending and receiving e-mails, and social media use (The Shift Project, 2021). These tools usually ask the user to enter information such as internet usage time, device type, data download and upload amount, e-mail traffic, and provide a digital carbon footprint estimate based on this data. For example, The Shift Project's "1byte" model helps estimate the carbon footprint of viewing a web page, sending an e-mail, or watching a video.

These calculators can be useful for raising awareness about the environmental impacts of digital technologies, supporting individual and corporate carbon footprint reduction efforts, developing more sustainable digital habits (e.g., lowering video resolution, deleting unnecessary e-mails, using devices for longer), choosing more environmentally friendly digital services (e.g., choosing data centers that use renewable energy), and informing policymakers.

However, it should be noted that the results of these calculators can vary significantly depending on the data used, assumptions, emission factors, and calculation methods, and usually provide an estimate or an "order of magnitude" estimate rather than a certainty. Different calculators may give different results for the same activity. Therefore, the results of these tools should be evaluated with a critical perspective.

Data Center Efficiency Metrics

Data centers are high-energy-density facilities that are at the heart of the modern digital economy, storing, processing, and distributing large amounts of data. These facilities consist of servers, storage systems, network equipment, cooling systems, power distribution units, and other supporting infrastructure. A number of standard metrics and best practices have been developed to evaluate, monitor, and improve the environmental impacts (especially energy consumption and water consumption) of data centers.

The most commonly used of these is Power Usage Effectiveness (PUE). PUE was first defined by The Green Grid consortium in 2007 and has since become the industry standard for measuring data center energy efficiency (The Green Grid, 2016). PUE is calculated as the ratio of the total energy consumption of a data center (all energy use of the facility, i.e., including lighting, cooling, power distribution) to the energy consumption of the IT equipment (servers, storage, network).

$$\text{PUE} = \frac{\text{Total Facility Energy Consumption}}{\text{IT Equipment Energy Consumption}}$$

An ideal PUE value is 1.0, meaning that all energy entering the data center is used directly by the IT equipment, with no energy loss in supporting systems such as cooling and power distribution. However, in the real world, PUE values typically range from 1.2 to 2.0 and can even be 3.0 or higher in some older and inefficient data centers. A lower PUE value indicates a more energy-efficient data center. Large technology companies such as Google, Facebook, and Microsoft are making significant investments to reduce their PUE values to 1.1 or lower.

Another important metric is Water Usage Effectiveness (WUE). WUE was first defined by The Green Grid in 2011 (Azevedo, 2011). WUE is calculated as the ratio of a data center's annual water use (in liters) to the energy consumption of the IT equipment (in kWh).

$$\text{WUE} = \frac{\text{Annual Water Use (Liters)}}{\text{IT Equipment Energy Consumption (kWh)}}$$

WUE is particularly important for evaluating and reducing the water footprint of data centers in regions with water scarcity or pressure on water resources. Data centers can use large amounts of water to cool servers (especially if evaporative cooling systems are used). To reduce WUE, methods such as water-saving cooling technologies (e.g., air-cooled systems, closed-loop cooling systems, free cooling), rainwater harvesting, and gray water reuse can be used.

In addition to PUE and WUE, there are other metrics such as Data Center Infrastructure Efficiency (DCiE), Carbon Usage Effectiveness (CUE), and Energy Reuse Factor (ERF). These metrics help data center operators monitor energy and water efficiency, identify areas for improvement, reduce costs, reduce environmental impacts, and achieve sustainability goals.

Challenges and Uncertainties

Measuring the digital carbon footprint accurately, comprehensively, and comparably faces a number of significant challenges and uncertainties. These challenges can be both technical and methodological, as well as related to data access and transparency.

One of the main challenges is the lack of data transparency. Many companies (especially technology companies, telecommunication operators, data center providers) do not fully disclose critical data such as energy consumption (electricity, fuel), water use, e-waste generation, supply chain emissions (Scope 3 emissions), and renewable energy use, do not report them in a standardized way, or do not have them independently verified (Van Heddeghem et. al., 2014). This situation makes it extremely difficult to obtain a holistic, transparent, and reliable picture of the environmental impacts of the digital sector and to compare the environmental performance of different companies or products. Although voluntary initiatives and regulations on corporate environmental, social, and governance (ESG) reporting (e.g., the European Union's Corporate Sustainability Reporting Directive - CSRD) are steps to improve this situation, significant shortcomings remain.

In addition, the supply chains of digital technologies are quite complex, spread globally, and involve a large number of different actors (raw material suppliers, component manufacturers, assemblers, distributors, retailers). The fact that hundreds, even thousands, of different components (semiconductors, displays, batteries, plastics, metals, etc.) used in the production of a smartphone, a laptop, or a server are supplied from dozens of different countries, and that the production process of each of these components has different environmental impacts (greenhouse gas emissions, water pollution, toxic waste, habitat destruction) makes it extremely difficult to accurately track, calculate, and report indirect emissions (Scope 3 emissions) (Andrae, 2020). Supply chain emissions often make up a large portion of a company's total carbon footprint (in some cases more than 80%), but measuring and reducing these emissions is much more difficult than directly controlled emissions (Scope 1 and Scope 2).

Other challenges include rapidly evolving technology (new devices, new applications, new business models), increasing data traffic (video streaming, cloud computing, Internet of Things), uncertainties in user behaviors (internet usage time, device usage frequency, energy saving habits), the use of different methodologies and assumptions (LCA, carbon footprint calculators), and uncertainties in future projections (the speed of technological developments, changes in the energy mix, climate change impacts).

These uncertainties and challenges make it difficult to develop effective policies and strategies to reduce the digital carbon footprint, to ensure that companies and individuals fulfill their environmental responsibilities, and to move towards a more sustainable digital future. Therefore, greater data transparency, standardized measurement and reporting methods, supply chain collaboration, and the joint efforts of policymakers, companies, researchers, and consumers are needed.

4. STRATEGIES FOR REDUCING DIGITAL CARBON FOOTPRINT

4.1. Individual Level

The steps individuals can take to reduce their digital carbon footprint can often have significant impacts with small changes in their daily digital habits. These changes include device usage, internet usage, e-mail and cloud storage habits, and adopting a more conscious digital consumption approach in general.

Device Usage

Device usage is a significant component of the individual digital carbon footprint. Simple measures that can be taken to reduce the energy consumption of devices include using the energy-saving mode of devices, lowering screen brightness (especially not using unnecessarily high brightness in bright environments), turning off devices completely when not in use (instead of leaving them in standby mode), and choosing longer-lasting, energy-efficient devices (e.g., Energy Star certified products) (EPA, 2024; Koomey & Masanet, 2021). In addition, extending the lifespan of devices reduces the frequent purchase of new devices, which helps to reduce the carbon footprint in the production phase. This means using devices carefully, evaluating repair options, and preferring second-hand devices if possible.

Internet Usage

Internet usage, especially data-intensive activities such as video streaming, online games, and downloading large files, causes significant energy consumption and therefore carbon emissions. To reduce these impacts, measures such as lowering video resolution (e.g., watching 1080p or 720p instead of 4K), avoiding unnecessary downloads and automatic playbacks, using ad blockers (ads also consume data and energy), and using a wired connection instead of Wi-Fi when possible (wired connection is generally more energy efficient) can be taken (The Shift Project, 2018; Freitag et. al., 2021). In addition, conscious internet use may include broader behavioral changes such as avoiding unnecessarily long periods of time online and digital detox.

E-mail and Cloud

E-mails and cloud storage services can have a larger carbon footprint than they appear. Simple steps such as unsubscribing from unnecessary e-mails, using spam filters effectively, using file-sharing links instead of sending large attachments (large attachments mean more storage space and therefore more energy consumption in both the sender's and recipient's mailboxes), regularly cleaning cloud storage and deleting unnecessary files (every file stored in the cloud takes up space on energy-consuming servers in data centers) can help reduce the carbon footprint in this area (Berners-Lee, 2020; Obringer et. al., 2021).

Conscious Consumption

Conscious digital consumption involves being aware of the environmental impacts of digital services and products, evaluating options to reduce these impacts, and choosing more sustainable alternatives. This may mean researching the environmental policies and practices of digital service providers (e.g., social media platforms, video streaming services, cloud storage providers), preferring companies with data centers that use renewable energy, questioning the environmental impacts of the materials and production processes used in the production of digital devices, and choosing less energy-consuming, longer-lasting, and recyclable products.

4.2. Corporate Level

Companies have a much greater responsibility than individuals to reduce their digital carbon footprint. Companies should prioritize energy efficiency and sustainability at every stage of their operations (from data centers to office buildings, from supply chains to product life cycles).

Green Data Centers

Data centers are at the heart of the digital economy and consume large amounts of energy. Therefore, increasing the energy efficiency of data centers and transitioning to renewable energy sources is one of the most important steps in reducing the corporate digital carbon footprint. This includes investing in renewable energy sources (solar, wind, hydroelectric, geothermal), using energy-efficient cooling systems (e.g., free cooling, liquid cooling, AI-powered cooling optimization), implementing server virtualization and optimization techniques (managing more workloads with fewer servers), recovering and reusing waste heat (e.g., using it to heat buildings), and regularly modernizing data center infrastructure (Barroso & Hölzle, 2007; Koomey, 2011; The Green Grid, 2016).

Sustainable Software Development

Software development processes can also be optimized in terms of energy consumption and carbon emissions. This includes approaches such as writing energy-efficient code (using algorithms that require less processing power and memory), adopting "Green AI" practices (reducing the amount of energy required to train and run artificial intelligence models), considering the energy consumption of the hardware on which the software runs, and designing user interfaces according to energy efficiency principles (Patterson et. al., 2021; Schwartz et. al., 2020).

Circular Economy

Adopting circular economic principles is an important way to reduce the environmental impacts of digital devices and infrastructure. This includes steps such as extending the life of devices (e.g., making modular designs, facilitating repair, providing software updates for a long time), promoting the recycling and reuse of devices (e.g., implementing take-back programs, selling refurbished devices), improving electronic waste management (preventing the release of toxic substances into the environment, recovering valuable metals), and promoting circular economy practices in the supply chain (MacArthur, 2013; Stahel, 2016).

4.3. Policies and Regulations

Governments and international organizations have an important role to play in reducing the digital carbon footprint. This may include various policies and regulations such as setting energy efficiency standards, implementing carbon taxes and incentives, requiring companies to report their emissions, supporting renewable energy investments, promoting circular economy practices, and strengthening international cooperation.

Energy Efficiency Standards: Governments can set minimum energy efficiency standards for digital devices (e.g., computers, servers, network equipment) and regularly update these standards. This encourages manufacturers to design more energy-efficient products.

Carbon Taxes and Incentives: Taxing carbon emissions encourages companies to reduce their emissions, while incentives for renewable energy and energy efficiency projects (e.g., tax breaks, subsidies) can increase investments in this area.

Emission Reporting Obligation: Requiring companies to regularly report their greenhouse gas emissions (Scope 1, Scope 2, and Scope 3) and have these reports independently verified increases transparency and encourages companies to take steps to reduce their emissions.

International Cooperation: The digital carbon footprint is a global problem, and combating this problem requires international cooperation. Countries can cooperate on issues such as information and technology sharing, developing common standards, and climate finance.

5. CASE STUDIES AND SUCCESS STORIES

Efforts to reduce the digital carbon footprint are supported by concrete examples at both the corporate level and at the individual and national levels. These case studies and success stories offer inspiring examples in a wide range, from renewable energy use to sustainable product design and policy regulations.

Green Data Centers

Data centers form the basis of the energy-intensive infrastructure of the digital world. Therefore, the efforts of large technology companies to make data centers more sustainable have a significant impact across industry.

Google: Google claims to have been carbon neutral since 2007 and to have used 100% renewable energy for its operations since 2017 (Google, 2020). The company invests heavily in renewable energy projects, uses artificial intelligence and machine learning to improve the energy efficiency of its data centers, and develops waste heat recovery projects. Google aims to operate on 24/7 carbon-free energy by 2030, meaning that all of its data centers and offices will be powered by local, carbon-free energy sources at all times of the day (Google, 2020).

Microsoft: Microsoft states that it has been carbon neutral since 2012 and aims to use 100% renewable energy by 2025 (Microsoft, 2020). The company makes renewable energy purchase agreements (PPAs), develops innovative cooling technologies (e.g., submarine data centers) to reduce water use in data centers, and invests in carbon capture and storage technologies. Microsoft aims to be carbon negative by 2030, meaning that the amount of carbon it removes from the atmosphere will be more than the amount of carbon it emits, and by 2050, the company plans to remove all the carbon it has emitted since its founding in 1975 from the atmosphere (Microsoft, 2020)2.

Apple: Apple states that it has reduced CO_2e emissions by over 55% in our carbon footprint since 2015 and aims for its supply chain to be carbon neutral by 2030 (Apple, 2024). The company invests in renewable energy projects such as solar farms, wind turbines, and biogas fuel cells, uses recycled materials in its products, and encourages its suppliers to switch to renewable energy.

Sustainable Practices

Some companies are developing innovative business models and products that support environmental sustainability using digital technologies.

Ecosia: Ecosia is a search engine that allocates a large portion of its profits to tree planting projects (Ecosia, 2025). Users contribute to tree planting with every search they make using Ecosia. Ecosia regularly publishes transparency reports, disclosing how much revenue it has generated, how much of this revenue has been allocated to tree planting, and which projects have been supported.

Fairphone: Fairphone is a smartphone produced ethically and sustainably (Fairphone, 2023). The company focuses on providing fair working conditions, avoiding conflict minerals, using recycled materials, extending the life of devices by making modular designs, and finding solutions to the electronic waste problem.

Country Examples

Some countries are adopting ambitious policies and practices to reduce the environmental impacts of the digital sector.

Iceland: Iceland, with its abundant renewable energy sources such as geothermal and hydroelectric power, is becoming an attractive location for data centers. The country's cool climate also reduces the cooling costs of data centers. Iceland aims to operate its data centers with 100% renewable energy and make its digital sector more sustainable (Government of Iceland, 2025).

Sweden: Sweden taxes the energy consumption of data centers and uses the revenue from this tax to support energy efficiency projects. In addition, the Swedish government has developed a national strategy to reduce the carbon emissions of the digital sector (Government Offices of Sweden, 2025).

France: France is working on various regulations to reduce the environmental impacts of the digital sector. These regulations aim to inform consumers about the energy consumption and carbon footprint of digital devices, increase the repairability of electronic devices, and promote the recycling of electronic waste. In addition, there are proposals in France to tax the carbon emissions of digital services (The Shift Project, 2020).

6. LOOKING TO THE FUTURE: CHALLENGES AND OPPORTUNITIES

The rapid evolution of digital technologies presents both challenges and opportunities for reducing the digital carbon footprint. While technological advancements hold potential for energy efficiency and optimization, raising societal awareness and shifting consumer behaviors are equally critical. However, ethical and social issues such as the digital divide, environmental justice, and data privacy and security must also be addressed.

Technological Developments

Technological innovations could become a key driver in reducing the digital carbon footprint.

Energy-Efficient Chips and Hardware

Microchips and other hardware components are primary determinants of energy consumption in digital devices. Developing chips and hardware that consume less energy has significant potential to reduce the digital carbon footprint. This can be achieved through innovative approaches such as shrinking transistor sizes (continuing Moore’s Law), using new materials (e.g., graphene, carbon nanotubes), 3D chip designs, neuromorphic (brain-inspired) chips, and photonic (light-based) chips (Shalf, 2020).

Energy Optimization with Artificial Intelligence (AI)

AI and machine learning (ML) are increasingly used to optimize energy consumption. In data centers, AI/ML algorithms can predict server workloads, optimize cooling systems, manage energy resources more efficiently, and even predict equipment failures to prevent energy waste (Ahmad, 2021; Patterson et al., 2021). AI/ML can also optimize energy distribution in smart grids, reduce energy consumption in buildings, and personalize energy usage for individual devices.

Quantum Computing Potential

Quantum computers have the potential to solve problems too complex for classical computers, revolutionizing fields like drug discovery, financial modeling, AI, and logistics. Certain algorithms could run on quantum computers with significantly less energy than traditional computers (Gyongyosi & Imre, 2019). However, widespread adoption and realizing the full energy efficiency potential of quantum computing will require substantial time and technological advancements.

Societal Awareness

Technological progress alone is insufficient. Reducing the digital carbon footprint demands increased societal awareness and changes in consumer behavior.

Improving Digital Literacy and Environmental Awareness

Educating individuals and institutions about the environmental impacts of digital technologies can foster more sustainable digital habits. Strategies include integrating environmental awareness into digital literacy programs, expanding access to digital carbon footprint calculators, encouraging transparent corporate sustainability reporting, and increasing media coverage of these issues (Freitag et al., 2021).

Shifting Consumer Behavior

Behavioral changes—such as choosing energy-efficient devices, using digital services more consciously, avoiding unnecessary data consumption, and practicing digital detox—can significantly reduce the digital carbon footprint. These changes can be supported by campaigns promoting sustainable digital lifestyles, educational materials, and applications leveraging behavioral economics principles (e.g., defaulting devices to energy-saving modes).

Ethical and Social Challenges

Efforts to reduce the digital carbon footprint raise ethical and social concerns that must be addressed.

The Digital Divide and Environmental Justice

Inequities in access to digital technologies (the digital divide) exacerbate environmental justice issues. Low-income communities and developing nations often rely on older, energy-inefficient devices and are disproportionately affected by the environmental impacts of digital technologies (e.g., pollution from e-waste). Policies to reduce the digital carbon footprint must include measures to bridge the digital divide and ensure environmental justice (Hernandez, 2019).

Data Privacy and Security

Some technologies aimed at reducing the digital carbon footprint (e.g., AI-driven energy optimization) require extensive data collection and analysis, raising concerns about data privacy and security. Striking a balance between energy efficiency and data privacy is critical. Transparent data collection practices and ensuring individuals retain control over their data are essential (Benthall et al., 2020; Hilty & Aebischer, 2015).

REFERENCES

Accounting, A. C. (2004). The Greenhouse Gas Protocol. World Resources Institute and World Business Council for Sustainable Development: Washington, DC, USA.

Afzal, S., Mehran, N., Ourimi, Z. A., Tashtarian, F., Amirpour, H., Prodan, R., & Timmerer, C. (2024). A Survey on Energy Consumption and Environmental Impact of Video Streaming. arXiv preprint arXiv:2401.09854. doi: 10.48550/arXiv.2401.09854.

Agiwal, M., Roy, A., & Saxena, N. (2023). Next generation 5G wireless networks: A comprehensive survey. IEEE Communications Surveys & Tutorials, 25(3), 1617-1655. doi: 10.1109/COMST.2016.2532458.

Ahmad, T., Zhang, D., Huang, C., Zhang, H., Dai, N., Song, Y., & Chen, H. (2021). Artificial intelligence in sustainable energy industry: Status Quo, challenges and opportunities. Journal of Cleaner Production, 289.

Akenji, L., Bengtsson, M., Toivio, V., Lettenmeier, M., Fawcett, T., Parag, T., ... & Kenner, D. (2021). 1.5-degree lifestyles: Towards a fair consumption space for all. Hot or Cool.

Andrae, A. (2020). New perspectives on internet electricity use in 2030. Engineering and Applied Science Letters, 3(2), 19-31. http://archive.bionaturalists.in/id/eprint/188.

Andrae, A. S. G., & Edler, T. (2015). On Global Electricity Usage of Communication Technology: Trends to 2030. Challenges, 6(1), 117-157. doi: 10.3390/challe6010117.

Andrews, J. G., Buzzi, S., Choi, W., Hanly, S. V., Lozano, A., Soong, A. C., & Zhang, J. C. (2014). What will 5G be?. IEEE Journal on selected areas in communications, 32(6), 1065-1082. doi: 10.1109/JSAC.2014.2328098.

Apple. (2024). Environmental Progress Report. Retrieved from (https://www.apple.com/environment/pdf/Apple_Environmental_Progress_Report_2024.pdf), on (15.02.2025).

Azevedo, D., Belady, S. C., & Pouchet, J. (2011). Water usage effectiveness (WUE): A green grid datacenter sustainability metric. The Green Grid, 32.

Baldé, C. P., Forti, V., Gray, V., Kuehr, R., & Stegmann, P. (2017). The Global e-waste Monitor 2017: Quantities, Flows and Resources. United Nations University, International Telecommunication Union, and International Solid Waste Association.

Benthall, S., & Goldenfein, J. (2020). Data Science and the Decline of Liberal Law and Ethics. doi: 10.2139/ssrn.3632577.

Barroso, L. A., & Hölzle, U. (2007). The case for energy-proportional computing. Computer, 40(12), 33-37.

Batmunkh, A. (2022). Carbon footprint of the most popular social media platforms. Sustainability, 14(4), 2195. doi: 10.3390/su14042195.

Belkhir, L., & Elmeligi, A. (2018). Assessing ICT global emissions footprint: Trends to 2040 & recommendations. Journal of Cleaner Production, 177, 448-463. doi: 10.1016/j.jclepro.2017.12.239.

Berners-Lee, M. (2020). How bad are bananas?: The carbon footprint of everything. Profile Books.

Borgia, E., Gomes, D. G., Lagesse, B., Lea, R., & Puccinelli, D. (2016). Special issue on "Internet of Things: Research challenges and Solutions". Computer Communications, 89, 1-4. doi: 10.1016/j.comcom.2016.04.024.

Carbonfootprint.com. Carbon footprint calculator. Retrieved from (https://www.carbonfootprint.com/calculator.aspx), on (15.02.2025).

Cahyaningrum, Y., Asif, M., Ihsan, A., & Rezki, Z. (2025). Sustainability and Ethics in Information Systems. Journal of Information Systems and Technology Research, 4(1), 13-21.

Cordella, M., Alfieri, F., & Sanfelix, J. (2021). Reducing the carbon footprint of ICT products through material efficiency strategies: A life cycle analysis of smartphones. Journal of Industrial Ecology, 25(2), 448-464. doi: 10.1111/jiec.13119.

Coroama, V. C., & Hilty, L. M. (2014). Assessing Internet energy intensity: A review of methods and results. Environmental Impact Assessment Review, 45, 63-68. doi: 10.1016/j.eiar.2013.12.004.

Curran, M. A. (2006). Life-cycle assessment: principles and practice. National Risk Management Research Laboratory, Office of Research and Development, US Environmental Protection Agency.

de Vries, A. (2018). Bitcoin's growing energy problem. Joule, 2(5), 801-805.

Ecosia. (2025). About Ecosia. Retrieved from (https://info.ecosia.org/), on (15.02.2025).

EPA. (2024). Greenhouse Gas Equivalencies Calculator. Retrieved from (https://www.epa.gov/energy/greenhouse-gas-equivalencies-calculator), on (15.02.2025).

Ericsson. (2020). A Quick Guide to Your Digital Carbon Footprint. Retrieved from (https://www.ericsson.com/en/reports-and-papers/industrylab/reports/a-quick-guide-to-your-digital-carbon-footprint), on (15.02.2025).

Fairphone. (2023). Fairphone's Impact 2023. Retrieved from (https://www.fairphone.com/wp-content/uploads/2024/06/Fairphone-2023-Impact-Report-.pdf), on (15.02.2025).

Fettweis, G., & Alamouti, S. (2014). 5G: Personal mobile internet beyond what cellular did to telephony. IEEE Communications Magazine, 52(2), 140-145. doi: 10.1109/MCOM.2014.6736754.

Forti V., Baldé C.P., Kuehr R., & Bel G. (2020). The Global E-waste Monitor 2020: Quantities, flows and the circular economy potential. United Nations University (UNU)/United Nations Institute for Training and Research (UNITAR) – co-hosted SCYCLE Programme, International Telecommunication Union (ITU) & International Solid Waste Association (ISWA), Bonn/Geneva/Rotterdam. Retrieved from (https://ewastemonitor.info/wp-content/uploads/2020/11/GEM_2020_def_july1_low.pdf), on (15.02.2025).

Freitag, C., Berners-Lee, M., Widdicks, K., Knowles, B., Blair, G. S., & Friday, A. (2021). The real climate and transformative impact of ICT: A critique of estimates, trends, and regulations. Patterns, 2(9). doi: 10.1016/j.patter.2021.100340.

Gallersdörfer, U., Klaaßen, L., & Stoll, C. (2020). Energy consumption of cryptocurrencies beyond bitcoin. Joule, 4(8), 1843-1846. doi: 10.1016/j.joule.2020.07.013.

Gandhi, A. P., Padhi, B. K., Goel, K., Singh, A., Kansal, O. P., & Al-Ahdal, T. (2023). Impact of virtual continued medical education on carbon footprint and awareness of digital sobriety: A retrospective cross-sectional study among public health professionals in India. Frontiers in Public Health, 11, 1118685. doi: 10.3389/fpubh.2023.1118685.

Ge, M., Bangui, H., & Buhnova, B. (2018). Big data for internet of things: a survey. Future generation computer systems, 87, 601-614. doi: 10.1016/j.future.2018.04.053.

Geissdoerfer, M., Savaget, P., Bocken, N. M., & Hultink, E. J. (2017). The Circular Economy–A new sustainability paradigm?. Journal of cleaner production, 143, 757-768. https://doi.org/10.1016/j.jclepro.2016.12.048.

Google. (2020). 24/7 by 2030: Realizing a carbon-free future. Retrieved from (https://www.gstatic.com/gumdrop/sustainability/247-carbon-free-energy.pdf), on (15.02.2025).

Government of Iceland. (2025). Energy. Retrieved from (https://www.government.is/topics/business-and-industry/energy/), on (15.02.2025).

Government Offices of Sweden. (2025). Digital policy. Retrieved from (https://www.government.se/government-policy/digital-policy/), on (15.02.2025).

Guinée, J. B., Gorrée, M., Heijungs, R., Huppes, G., Kleijn, R., De Koning, A., ... & Suh, S. (2002). Handbook on life cycle assessment: Operational guide to the ISO standards. Springer Science & Business Media.

Gupta, A., & Jha, R. K. (2015). A Survey of 5G network: Architecture and emerging technologies. IEEE Access, 3, 1206-1232. doi: 10.1109/ACCESS.2015.2461602.

Gyongyosi, L., & Imre, S. (2019). A survey on quantum computing technology. Computer Science Review, 31, 51-71. doi: 10.1016/j.cosrev.2018.11.002.

Hilty, L. M., & Aebischer, B. (Eds.). (2015). ICT innovations for sustainability (Vol. 310). Cham: Springer International Publishing. doi: 10.1007/978-3-319-09228-7.

Hernandez, J. (2019). Indigenizing environmental justice: Case studies from the Pacific Northwest. Environmental Justice, 12(4), 175-181.

ISO. (2006). ISO 14040: 2006. Environmental Management—Life Cycle Assessment—Principles and Framework. International Organization for Standardization. Geneva.

ISO. (2006b). ISO 14044: 2006 Environmental Management — Life Cycle Assessment — Requirements and Guidelines. International Organization for Standardization. Geneva.

Itten, R., Hischier, R., Andrae, A. S., Bieser, J. C., Cabernard, L., Falke, A., ... & Stucki, M. (2020). Digital transformation—life cycle assessment of digital services, multifunctional devices and cloud computing. The International Journal of Life Cycle Assessment, 25, 2093-2098.

Jones, N. (2018). How to Stop Data Centres from Gobbling up the World’s Electricity. Nature, 561(7722), 163-166.

Kang, W., Zhu, D., Zhang, S., Liu, J., & Ma, R. (2025). A group scheduling algorithm for massive heterogeneous data in the “dual carbon” digital intelligence monitoring center considering time-varying characteristics and priorities. Sustainable Energy Research, 12(1), 4.

Kim, J., Ryu, D., & Sovacool, B. K. (2021). Critically assessing and projecting the frequency, severity, and cost of major energy accidents. The Extractive Industries and Society, 8(2), 100885.

Koomey, J. (2011). Growth in data center electricity use 2005 to 2010. A report by Analytical Press, completed at the request of The New York Times, 9(2011), 161.

Koomey, J. G., & Masanet, E. (2021). Does not compute: Avoiding pitfalls assessing the internet's energy and carbon impacts. Joule, 5(8), 1958-1962.

Köhler, S., & Pizzol, M. (2019). Life cycle assessment of Bitcoin mining. Environmental science & technology, 53(23), 13598-13606. doi: 10.1021/acs.est.9b05687.

MacArthur, E. (2013). Towards the circular economy, economic and business rationale for an accelerated transition. Ellen MacArthur Foundation: Cowes, UK, 1.

Masanet, E., Shehabi, A., Lei, N., Smith, S., & Koomey, J. (2020). Recalibrating Global Data Center Energy-Use Estimates. Science, 367(6481), 984-986. https://www.science.org/doi/10.1126/science.aba3758.

Microsoft. (2020). Microsoft Will Be Carbon Negative by 2030. Retrieved from (https://blogs.microsoft.com/blog/2020/01/16/microsoft-will-be-carbon-negative-by-2030/), on (15.02.2025).

Mills, E., Bourassa, N., Rainer, L., Mai, J., Shehabi, A., & Mills, N. (2019). Toward greener gaming: Estimating national energy use and energy efficiency potential. The Computer Games Journal, 8, 157-178.

Naeem, R., Kareem, W., & Naeem, B. (2023). Social Media Platforms and their Digital Carbon Footprints: Analyzing Awareness level of Social Media Users of Punjab, Pakistan. Int J Media Net, 1(1), 01-07. https://doi.org/10.21203/rs.3.rs-3299158/v1.

Nayeri, Z. M., Ghafarian, T., & Javadi, B. (2021). Application placement in Fog computing with AI approach: Taxonomy and a state of the art survey. Journal of Network and Computer Applications, 185, 103078. doi: https://doi.org/10.1016/j.jnca.2021.103078.

Nutanix. (2023). What Is a Digital Carbon Footprint & How Can You Reduce Yours? Retrieved from (https://www.nutanix.com/info/digital-carbon-footprint), on (15.02.2025).

O'Connell, S., & Stutz, M. (2010). Product Carbon Footprint (PCF) Assessment of Dell Laptop-Results and Recommendations. Proceedings of the 2010 IEEE International Symposium on Sustainable Systems and Technology, Arlington, VA, USA (pp. 1-6). https://doi.org/10.1109/ISSST.2010.5507731.

Obringer, R., Rachunok, B., Maia-Silva, D., Arbabzadeh, M., Nateghi, R., & Madani, K. (2021). The overlooked environmental footprint of increasing Internet use. Resources, Conservation and Recycling, 167(105389), 04.

Patterson, D., Gonzalez, J., Hölzle, U., Le, Q., Liang, C., Munguia, L. M., ... & Dean, J. (2021). Carbon emissions and large neural network training. arXiv preprint arXiv:2104.10350.

Pihkola, H., Nors, M., Kujanpää, M., Helin, T., Kariniemi, M., Pajula, T., Dahlbo, H., & Koskela, S. (2010). Carbon footprint and environmental impacts of print products from cradle to grave: Results from the LEADER project (Part 1). VTT Technical Research Centre of Finland. VTT Tiedotteita - Meddelanden - Research Notes No. 2560 https://publications.vtt.fi/pdf/tiedotteet/2010/T2560.pdf

R1234yf. (2024, February 10). In Wikipedia. https://en.wikipedia.org/wiki/2,3,3,3-Tetrafluoropropene.

Rebitzer, G., Ekvall, T., Frischknecht, R., Hunkeler, D., Norris, G., Rydberg, T., ... & Pennington, D. W. (2004). Life cycle assessment: Part 1: Framework, goal and scope definition, inventory analysis, and applications. Environment International, 30(5), 701-720. Doi: 10.1016/j.envint.2003.11.005.

Riabova, J. (2025). A Framework for Sustainable Web Design in the Era of Digital Transformation. In: Elstermann, M., Lederer, M. (eds) Subject-Oriented Business Process Management. Models for Designing Digital Transformations. S-BPM ONE 2024. Communications in Computer and Information Science, vol 2206. Springer, Cham. https://doi.org/10.1007/978-3-031-72041-3_13.

Salahuddin, M., and Alam, K. (2016). Internet usage, electricity consumption and economic growth in Australia: A time series evidence. Telematics and Informatics, 33(4), 1106-1120. doi: https://doi.org/10.1016/j.tele.2015.04.011.

Schwartz, R., Dodge, J., Smith, N. A., & Etzioni, O. (2020). Green AI. Communications of the ACM, 63(12), 54-63. doi: 10.1145/3381831.

Shalf, J. (2020). The future of computing beyond Moore’s Law. Philosophical Transactions of the Royal Society A, 378(2166). doi: 10.1098/rsta.2019.0061.

Shehabi, A., Smith, S. J., Horner, N., Azevedo, I. L., Masanet, E., & Koomey, J. (2016). United States data center energy usage report. https://escholarship.org/uc/item/84p772fc.

Stahel, W. R. (2016). The circular economy. Nature, 531(7595), 435-438. doi: 10.1038/531435a.

Stoll, C., Klaaßen, L., and Gallersdörfer, U. (2019). The carbon footprint of Bitcoin. Joule, 3(7), 1647-1661. doi: 10.1016/j.joule.2019.05.012.

T. A., S. M., D., R. D., & Repakula, R. (2025). Sustainable Creations: A Holistic Guide to Optimize Digital Footprints and Foster Climate-Conscious Innovation. In J. Mukthar K. P., V. Jain, S. Tsai, & C. Wu (Eds.), Digital Innovations for Renewable Energy and Conservation (pp. 313-330). IGI Global Scientific Publishing. https://doi.org/10.4018/979-8-3693-6532-8.ch013.

The Green Grid. (2016). Data Center Maturity Model (DCMM). Retrieved from (https://www.thegreengrid.org/en/resources/library-and-tools/438-Data-Center-Maturity-Model), on (15.02.2025).

The Shift Project. (2018). "Lean ICT: Towards Digital Sobriety": Our New Report on the Environmental Impact of ICT. Retrieved from (https://theshiftproject.org/en/article/lean-ict-our-new-report/), on (15.02.2025).

The Shift Project. (2020). "Lean ICT: Towards Digital Sobriety": A Responsible Corporate Approach. Retrieved from (https://www.cigref.fr/wp/wp-content/uploads/2020/12/Cigref-The-Shift-Project-Digital-Sobriety-A-responsible-corporate-approach-october-2020_EN.pdf), on (15.02.2025).

Weber, C. L., Koomey, J. G., & Matthews, H. S. (2010). The Energy and Climate Change Implications of Different Music Delivery Methods. Journal of Industrial Ecology, 14(5), 754-769. doi: 10.1111/j.1530-9290.2010.00269.x.

Widmer, R., Oswald-Krapf, H., Sinha-Khetriwal, D., Schnellmann, M., & Böni, H. (2005). Global perspectives on e-waste. Environmental Impact Assessment Review, 25(5), 436-458. https://doi.org/10.1016/j.eiar.2005.04.001.

Williams, E. (2011). Environmental Effects of Information and Communications Technologies. Nature, 479(7373), 354-358. https://doi.org/10.1038/nature10682.

Williams, L., Sovacool, B. K., & Foxon, T. J. (2022). The energy use implications of 5G: Reviewing whole network operational energy, embodied energy, and indirect effects. Renewable and Sustainable Energy Reviews, 157, 112033.

Watari, T., McLellan, B. C., Giurco, D., Dominish, E., Yamasue, E., & Nansai, K. (2019). Total material requirement for the global energy transition to 2050: A focus on transport and electricity. Resources, Conservation and Recycling, 148, 91-103. Zhou, X., Yao, L., & Zhang, Y. (2019). Energy consumption model and energy efficiency of video streaming for mobile devices. Tsinghua Science and Technology, 24(3), 319-331.

Van Geet, O., & Sickinger, D. (2024). Best practices guide for energy-efficient data center design (No. NREL/TP-5R00-89843). National Renewable Energy Laboratory (NREL), Golden, CO (United States).

Van Heddeghem, W., Lambert, S., Lannoo, B., Colle, D., Pickavet, M., & Demeester, P. (2014). Trends in worldwide ICT electricity consumption from 2007 to 2012. Computer Communications, 50, 64-76. doi: 10.1016/j.comcom.2014.02.008.

Zilio, C., Brown, J. S., Schiochet, G., & Cavallini, A. (2011). The refrigerant R1234yf in air conditioning systems. Energy, 36(10), 6110-6120. https://doi.org/10.1016/j.energy.2011.08.002.

CHAPTER 2

AWJ Machining of Polymers and Polymer Matrix Composites

Mustafa Armağan[1]

[1] Dr. Istanbul Medeniyet University, ORCID: 0000-0003-0429-0351

Introduction

Today, polymer and polymer matrix composite materials have a wide range of applications in the manufacturing industry. The machining of these materials differs from others (metals, etc.). The behavior of material varies according to matrix and fiber type, fiber orientation, distribution ratio in material, and so tool encounters constantly changing workpiece. In traditional machining methods, difficulties such as tool life, cost and production quality are encountered in machining with this variable material structure (Cenna & Mathew, 1997). Hard, abrasive and refractive components in material structure can provide to rapid wear of machining tools and material removing ratio is decreased. This negative situation is removed with alternative machining methods. Alternative methods name is basically non-traditional machining methods, which includes laser machining, electrical discharge machining, water jet and AWJ machining, ultrasonic machining, and electrochemical spark machining, et al. (Komanduri, 1997). Nontraditional machining methods achieves low cost and high quality for manufacturing goods, thus advantages of processes are very important and this methods are a developing options for manufacturers (Yao et al., 2005). Jain and Jain implied to advanced machining processes for nontraditional machining methods and this researchers reviewed to analytical models on mechanism of material removal of various advanced machining methods such as AWJ for previous studies (Jain & Jain, 2001). According to previous studies, Sureban et al. reviewed modern optimization techniques for various advanced machining methods (Electro Discharge Machining (WEDM), Laser Beam Machining (LBM), AWJ machining and Electro Discharge Machining (EDM). They concluded that less work was done on water jet machining process parameters optimization in the study (Sureban, Kulkarni, & Gaitonde, 2019). Temuçin et al. improved a fuzzy based decision model on selection to nontraditional machining method. In Figure 1, proposed decision support model was shown by researchers and for the cutting process (in the determined material and size) results were stated. According to results, water jet and abrasive water jet was best first and second machining methods, respectively (Temuçin, Tozan, Vayvay, Harničárová, & Valíček, 2014).

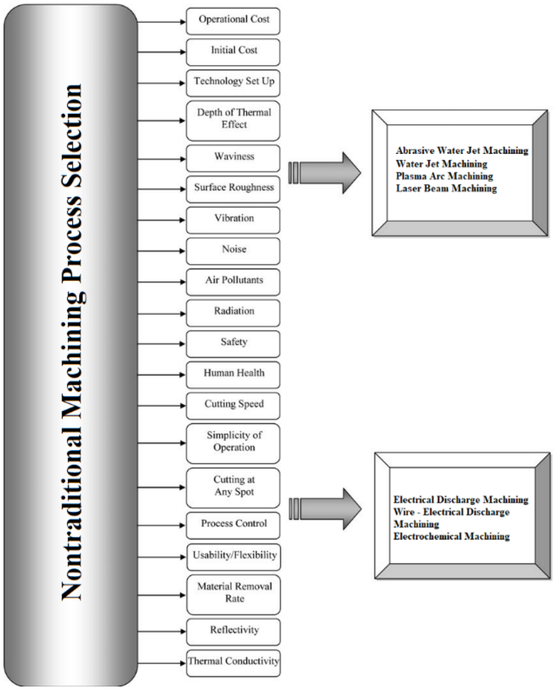

Figure 1. Visual of proposed decision support model (Temuçin et al., 2014)

General components of the abrasive water jet are shown in Figure 2(a) and 2(b). In Figure 2 (a), the hydraulic unit consists of an electrically operated hydraulic pump. Intensifier increases the water pressure coming from the pump and the accumulator or shock attenuator ensures that the incoming water pressure is smooth. Filters remove foreign substances that may come from water and thus filters guard the nozzle orifice. Water transmission lines include plumbing elements suitable in high pressure and the on / off valve typically switches the jet stream on or off. Abrasive water jet nozzle is where pressurized water and abrasive combine, and it sends on the combination to the target material. While abrasive water jet leaves the target material, it is ensured the capture and distribution of this jet by the water jet catcher (JACKSON C & OLSON RD, 1969). The modern configuration of all these processes is shown in Figure 2(b). According to the figure, the PC-based Controller is the element that manages the operations such as nozzle motion control and pressure adjustment to perform the designed machining. The abrasive hopper provides a specified amount of flow of abrasive material. And other elements are similar to the traditional AWJ workbench (‘AWJ machine’, 2020).

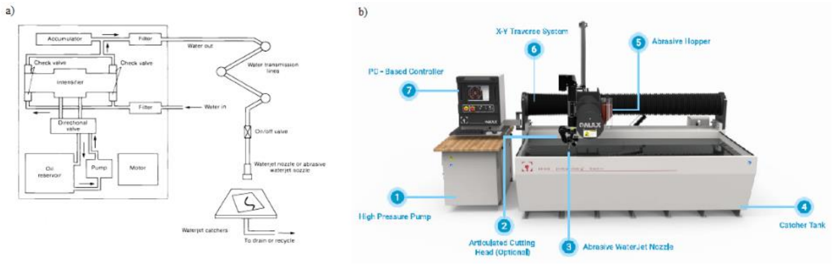

Figure 2. General components of the abrasive water jet (a) (JACKSON C & OLSON RD, 1969) and (b) ('AWJ machine', 2020)

The basic working principle of the abrasive water jet is based on mixture sent above of target material by driving, mixing and accelerating of the abrasive particles with pressured water. This acceleration and mixing processes are carried out in a mixing chamber and/or mixing tube which made from a hard material (Mohamed Hashish, 1984). Example configurations of the nozzles containing all these processes are shown in Figure 3 (a-c).

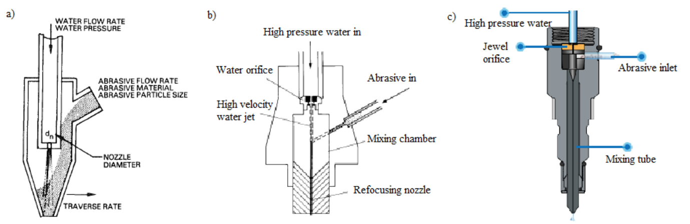

Figure 3. Example configurations of the nozzles (a) (Mohamed Hashish, 1984), (b) (JACKSON C & OLSON RD, 1969), (c) ('AWJ nozzle', 2020)

Factors affecting cutting performance in abrasive water jet are collected under four main headings. These are hydraulic, abrasive, mixing - acceleration and cutting parameters. According to Hashish (Mohamed Hashish, 1984, 1989) and Kechagias et al. (Kechagias, Petropoulos, & Vaxevanidis, 2012) studies, the arrangement of the four main headings with their sub-details were shown in Figure 4.

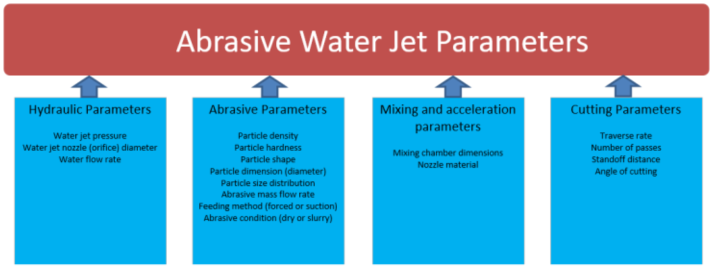

Figure 4. Abrasive water jet parameters

By abrasive water jet machining, the cutting surface mainly consists of Mode I and Mode II. Mode I is cutting wear mode; as in a micro processing process within the cutting wear zone, the material is removed by the particles impact at shallow angles. Mode II is deformation wear mode. In deformation wear zone, with the particles impact at large angles, it is characterized by the removal of material due to excessive plastic deformation (Ahmad, 2009; Mohamed Hashish, 1984, 1991; Mohamed, 1988). Cutting and deformation wear zones are shown in Figure 5 (a) and (b). In Arola and Ramulu works, they divided the cutting surface with abrasive water jet into three distinct surfaces (Figure 5 (b)). The initial damage region (IDR) occurs on the top the kerf. This phenomenon results from the slope of jet energy with radial distance and the jet expansion before impact. In this region, the abrasive attack angle is much larger according to the remaining cutting depth. The smooth cutting region (SCR) and the rough cutting region (RCR) are located under the IDR, and these two regions are distinguished by waviness patterns. The surface texture processed in the SCR is primarily determined by the abrasive particle size. In contrast, cutting parameters that affect the jet kinetic energy manage the surface properties of the RCR (Arola & Ramulu, 1997).

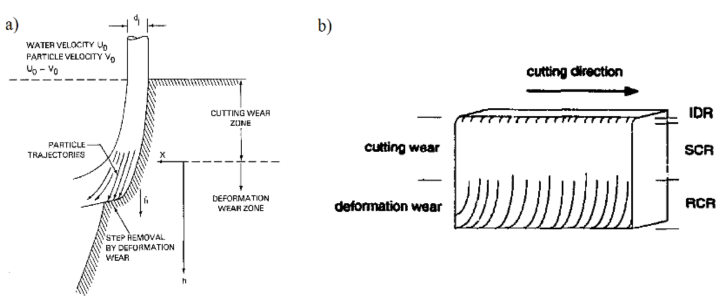

Figure 5. Cutting surface wear mechanisms: (a) (Mohamed Hashish, 1984), (b) (Arola & Ramulu, 1997)

In this study, the literature on the machining of polymers and polymer composites with abrasive water jet is examined in detail. All studies under the cutting process was reviewed. Then, the data was classified into tables and explanatory figures were added. Analysis of the literature has been made and targets for the future have been determined.

Cutting Studies

In literature, more than half of all work done was cutting process for polymer and polymer composites material by AWJ. Thus, AWJ machining is usually about cutting process. General factors of all the studies mentioned in this section were shown in Table 1. Detailed examination was made according to the content of Table 1, and thus comments were made. Hashish (Mohamed, 1988) worked to visualize AWJ cutting process. In the mentioned study, two types of transparent thermoplastic polymer plates were used and so cutting wear and deformation wear modes have been found. Under various experimental parameters, visualization of the cutting (entry, developed cutting et al.) stages were completed and especially conclusions of penetration rate and depth of cut with these parameters were expressed. With the increase in the particle size, the cutting wear zone affected negatively. Abrasive mass flow rate parameter has been stated to more affect to deformation wear zone. Ramulu and Arola (Ramulu & D.AROLA, 1992) cut unidirectional graphite/epoxy composite laminates with AWJ and water jet (WJ). Average surface roughness (R_a) values were found to be better with almost AWJ cutting and these values have generally changed according to fiber orientation. In another study (M. Hashish, Steele, & Bothell, 1997), various materials were cut at a pressure (up to 690 MPa) higher than conventional AWJ/WJ pressures. In addition, a polymer additive has been added to the cutting water. Higher traverse rate was thought to be required for delamination in plain fiberglass at higher pressure. Also, polymer additive increased the depth of cut at relatively low water jet pressure. In the study of Wang (Jun Wang, 1999), Teflon fabric/phenolic resin composite has been cut by abrasive water jet. According to study, kerf width and kerf taper angle increased with increase of water pressure and standoff distance parameters. But kerf taper angle and kerf width decreased mostly with increase of traverse speed parameter. Wang and Guo (J. Wang & Guo, 2002) cut Phenolic Fabric Polymer Matrix composite with abrasive water jet and they developed a semi-empirical model for polymer matrix composites. This model predicted depth of jet penetration. By design of experimental parameters all tests have been resulted, and it has been compared to the model with experimental values. As a result, depth of penetration increased with increase of water pressure and abrasive mass flow rate parameters, but this trend was inversely proportional to traverse speed. Lemma et al. (Lemma, Chen, Siores, & Wang, 2002a) investigated the effect of nozzle oscillation technique on the workpiece surface in AWJ cutting. The nozzle oscillation technique is performed by oscillating motion of nozzle head at the determined angle and frequency. Polymethylmethacrylate (PMMA) material has been cut to show the trace profile, and this situation was illustrated in Figure 6. According to oscillation technique with AWJ cutting, which was cut with a greater number of fresh abrasives water jets per unit time. Here, the effect of AWJ cutting with nozzle oscillation technique on beneficial trace profile have been observed.

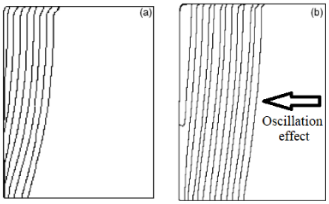

Figure 6. (a) Traditional AWJ cutting trace profile, (b) AWJ cutting trace profile by nozzle oscillation effect (Lemma et al., 2002a)

Lemma et al. (Lemma, Chen, Siores, & Wang, 2002b) examined the effect of nozzle oscillation on cutting glass fiber reinforced polymer composites with abrasive water jet. It has been stated that improvements in surface quality were better when levels of high oscillation angle and frequency were selected. Chen and Soirees (Chen & Siores, 2003) studied the striation formation on cutting surface with AWJ. The kinetic energy of the abrasive particles happened the most important effect on material removal rate. This striation formation has been advocated by abrasive particle kinetic energy distribution consisted in an undulating form and schematic description of striation formation mechanism was shown in Figure 7. In another study (J. Wang, Kuriyagawa, & Huang, 2003), phenolic fabric polymer matrix composite sheet has been cut by abrasive water jet. According to resulted depth of penetration and surface roughness values, optimum jet impact angle was found about at 80° angle has little effect on it.

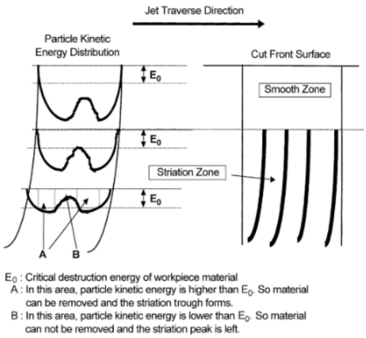

Figure 7. Striation formation mechanism according to particle kinetic energy distribution (Chen & Siores, 2003)

Deam et al. (Deam, Lemma, & Ahmed, 2004) worked on modeling cutting process with abrasive water jet. Verification of model created was done by visualization experiments and these experiments included PMMA material with AWJ cutting. As a result, it has been stated that models match well with experimental (visualisation) data in case of steady state cutting. Lemma et al. (Lemma, Deam, & Chen, 2005) investigated the effect of oscillation on the maximum depth of cut in the cutting process with abrasive water jet. For this investigation, visualization experiments of PMMA material have been used. Traces at jet solid interface relative to conventional and oscillation AWJ cutting were shown in Figure 8. According to experimental parameters in the figure, it has been interpreted that the maximum depth of cut will be in Figure 8(c) because the angle of traces was lowest, and frequency of traces was highest. Visualisation and parametric experiments results have been combined and thus a semi-empirical model was created.

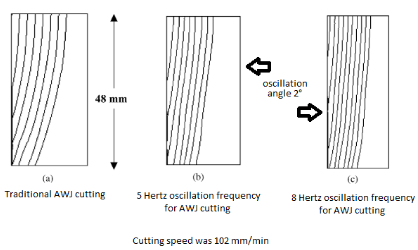

Figure 8. Traces of the jet/solid interface (a) traditional AWJ cutting (b) and (c) oscillation cutting with AWJ (Lemma et al., 2005)

Monno and Ravasio (Monno & Ravasio, 2005) investigated the effect of vibration on surface machined by AWJ. It has been stated in the study that vibration was divided into two as internal and external source. The internal source contained cutting head vibrations, the movement system and the intensifier system and these allowed the formation of the jet and affected it. As to the external source contained the interactions in air with the workpiece, the equipment and the water in the catcher and thus it caused vibration on the workpiece by the jet. All vibration experiments were done on rubber material. Consequently, if splash back damping fixing equipment and new-small diameter nozzle use, vibration frequency and amplitude with surface roughness will decrease. Ma and Deam (Ma & Deam, 2006) examined the variation of kerf widths (Figure 9(a)), which were formed when cutting acrylic material with abrasive water jet, according to various traverse speeds. After kerf widths measured, a correlation has been created. For example, as shown in Figure 9(b), this correlation showed two distinct regions. The first and second region were named developing stage and fully developed stage (after about 2 mm of the cutting depth), respectively. The developing stage referred to changing flow with initial contact of the jet on target material. The fully developed stage referred to the expansion or contraction of the kerf depending on the speed. In addition, different standoff distances were examined for variations of kerf width.

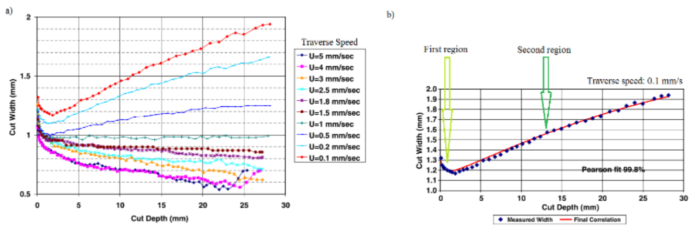

Figure 9. (a) Different traverse speed for kerf width (b) Correlation regions (Ma & Deam, 2006)

Orbanic and Junkar (Orbanic & Junkar, 2008) analyzed the striation mechanism formed on cutting surface during AWJ cutting process. According to study, oscillation of the jet was detected in AWJ cutting of PMMA and then two phenomena were introduced for the striation formation mechanism. These two phenomena were expressed as river meandering and wear of the pneumatic conveyor bends. The schematic view of striation formation was shown in Figure 10.

Azmir and Ahsan (Azmir & Ahsan, 2008) cut the glass/epoxy composite laminates with AWJ according to various parameters so cutting surface investigated for surface roughness. After Taguchi experimental design was constituted, analysis of variance (ANOVA) performed. In addition, the effect of noise factors was inspected. For R_a consequently, type of abrasives, pressure and traverse rate were significant control factors also form of fibres and thickness of laminate were important noise factors.

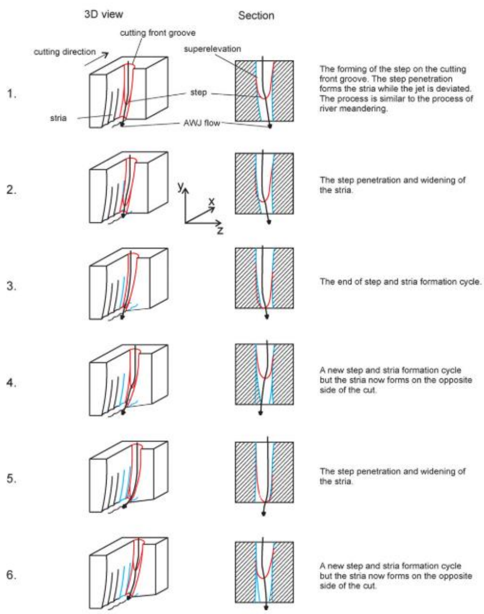

Figure 10. Schematic view of striation formation (Orbanic & Junkar, 2008)

Shanmugam et al. (Shanmugam, Nguyen, & Wang, 2008) investigated delamination that can occur in the cutting of graphite epoxy composite laminates by AWJ. The schematic view of the delamination mechanism proposed according to various experimental studies was shown in Figure 11. During the delamination process (Figure 11(a)), primarily formation of the fracture was observed under the influence of the jet's inlet. Afterwards, it has been explained that water-wedging (Figure 11(b) and abrasive embedment (Figure 11(c)) were formed respectively. In addition, the predictive delamination model developed and thus the maximum crack length was estimated. Azmir and Ahsan (Azmir & Ahsan, 2009) examined the AWJ cutting performance of glass-epoxy composite laminate. According to Taguchi experimental design and ANOVA analysis investigated for R_a and kerf taper ratio (T_R). Pressure, standoff distance, cutting orientation and abrasive mass flow rate were significant experimental parameters for R_a, respectively. Abrasives type, standoff distance and traverse rate were significant parameters for T_R, respectively. In conclusion, optimum experimental parameters and their levels obtained for R_a and T_R.

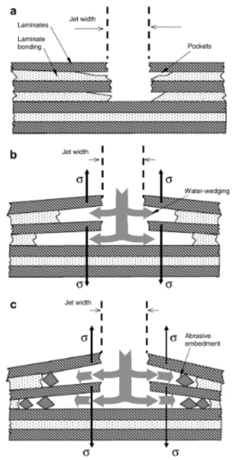

Figure 11. The schematic view of the delamination mechanism (a) formation of the fracture, (b) water-wedging, (c) abrasive embedment (Shanmugam et al., 2008)

Shanmugam and Masood (Shanmugam & Masood, 2009) cut two different polymer matrix composite laminates by abrasive water jet and cutting surface has been investigated for kerf taper angle. These composite materials were epoxy pre-impregnated graphite woven fabric and glass epoxy. According to researchers, when high pressure, low traverse speed and low standoff distances were selected, kerf taper angle was minimum for both composites. Also, a semi-analytical model specific to this experiment and composites were derived. Azmir et al. (Azmir, Ahsan, & Rahmah, 2009) examined the effects of test parameters on R_a and T_R in abrasive water jet cutting of aramid fiber reinforced composite material. After all tests performed according to Taguchi experimental design, ANOVA analysis realized. Traverse rate and pressure were significant experimental parameters for R_a, respectively. Traverse rate and standoff distance were significant parameters for T_R, respectively. After regression equations for R_a and T_R were found, predicted results according to these equations and experimental results were compared. Hlaváč et al. (Hlaváč et al., 2009) examined the declination angle according to thickness and traverse speed in cutting of various materials such as PMMA, red plastic and yellow plastic with abrasive water jet. For limit traverse speed an equation was modified considering that traverse speed and declination angle(s). In addition, experimental verification of limit traverse speed has been performed. In the other stage of the study, traverse speed was found according to determined declination angle for all materials, and these values were compared experimentally. It was stated that the trailback of the jet can be reduced on the cutting surface when the cutting head was tilted to half of targeted the declination angle. Siddiqui and Shukla (Siddiqui & Shukla, 2010) have developed a semi-empirical model on the prediction of the cutting depth in the cutting of the Kevlar-epoxy composite with abrasive water jet. Predicted and experimental depth of cut values have been found and these values compared. In addition, the effects of parameters and parameter levels on the depth of cut were expressed. Zhenglong (Zou, 2012) investigated the effect of low pressure in cutting of glass fiber and carbon fiber reinforced plastics with pre-mixed abrasive water jet. The effect of test parameters and parameter levels on the depth of cut was observed by ANOVA analysis. As a result, it was stated that injection pressure was one of the main parameters affecting the cutting quality. Stoić et al. (Stoić, Duspara, Kosec, Stoić, & Samardžić, 2013) examined the polyamide 6 cutting with abrasive water jet. Surface roughness was measured along the depth of cut according to various test parameters and parameter levels. Alberdi et al. (Alberdi, Suárez, Artaza, Escobar-Palafox, & Ridgway, 2013) have found machinability indexes in cutting of two kinds carbon fiber reinforced composite materials with AWJ and then the effects of experimental parameters on the taper angle and surface roughness were investigated. The machinability index of composite materials was found higher than materials such as aluminum 2024 and stainless steel 316 so it has been stated that composite materials can be cut faster than metals. In addition, the workability index of two types of materials was found to be different. It was interpreted that this difference can be caused by fibre volume content and/or tensile modulus values. According to the ANOVA analysis, thickness and traverse rate parameters were found significantly for taper angle and surface roughness, respectively. Effect of experimental parameters on delamination formation in cutting of carbon fiber reinforced plastics with AWJ has been investigated (Mayuet et al., 2015). In the mentioned study, delamination formations have been characterized with Scanning Optical Microscope (SOM) and Scanning Electron Microscope (SEM). On cutting surface, the embedding of abrasive particles in the fiber delamination and entrance of abrasive particles into the layers were shown in Figure 12(a) and Figure 12(b), respectively. As a result, it has been stated that the abrasive was the most effective parameter on delamination formation.

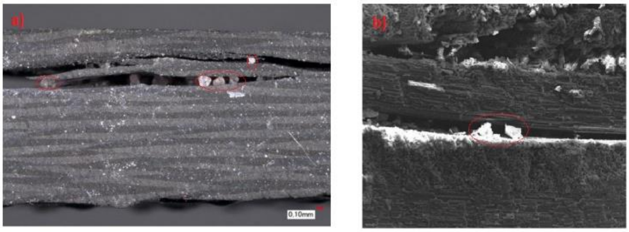

Figure 12. (a) embedding of abrasive particles in the fiber delamination (SOM image), (b) entrance of abrasive particles into the layers (SEM image) (Mayuet et al., 2015)

Li et al. (R. Li et al., 2015) have investigated the effect of experimental parameters on surface roughness in cutting recombinant bamboo with AWJ. Phenol formaldehyde resin adhesive was used in the production of recombinant bamboo. And this material has been produced in two different thicknesses also the orientation effect (various cutting direction) of the composite was investigated for surface roughness according to the experimental parameters. A Box-Behnken experimental design has been provided according to response surface methodology. For all test conditions, the surface roughness generally increased when feed rate and abrasive mass flow rate increased, but as pressure increases, the surface roughness was generally decreased. Ramesha et al. (Narayanappa Ramesha, 1 Siddaramaiah, 2016) have worked in cutting of banyan tree powder (with /without maleic anhydride grafted polypropylene (PP-g-MA) or talc) filled polypropylene composite with abrasive water jet. When traverse speed increased, kerf taper angle mostly increased. This trend was expressed by the decrease in the number of abrasive particles that penetrate the composites due to the increase in traverse speed. In addition, it stated that with the addition of the coupling agent PP-g-MA, it increased the adhesion of the interface between matrix and composite, thereby surface roughness has been reduced. Hu et al. (Hu, Tang, Kang, & Li, 2016) added the polyacrylamide polymer to abrasive water jet cutting water and thus with the addition of this polymer, they investigated the cutting performance of the marble. At the concentration of about 600 ppm of polyacrylamide, minimum kerf taper angle was found. The polymer addition (600 ppm) along the depth of cut has produced a better surface roughness. The improvement of polyacrylamide additive on cutting surface was shown in Figure 13. According to Figure 13, the deformation wear zone length has been shortened with the addition of polyacrylamide and as a result, it has been stated that the cutting quality has improved.

Figure 13. (a) Cutting surface without polyacrylamide solution, (b) cutting surface with polyacrylamide solution (600 ppm) (Hu et al., 2016)

Dhanawade et al. (Dhanawade, Kumar, & Kalmekar, 2016) investigated the cutting of the carbon epoxy composite with AWJ. The cuttings have been made according to the Taguchi experimental design, and the effects on surface roughness and kerf taper angle of experimental parameters were determined by ANOVA analysis. In ANOVA analysis, it was stated that the most significant parameters for surface roughness and kerf taper angle were pressure and traverse rate, respectively. As pressure was increased surface roughness and kerf taper angle was decreased. Also, as the traverse rate was increased, surface roughness and kerf taper angle were increased. Jani et al. (Jani, Kumar, Khan, & Kumar, 2016) investigated effect of the experimental parameters and the fillers on the cutting surface in cutting of hemp-Kevlar fibers (with and without palm shell and coconut shell fillers) epoxy composite material with AWJ. After L9 orthogonal test array selected, the experiments have been carried out at three factors (jet pressure, traverse speed, and standoff distance) and three levels. When the effect of filler materials was examined, the effect rates of these factors for kerf inclination, material removal rate and surface roughness response parameters generally showed similar behavior. Traverse speed was the most (by far) efficient factor for surface roughness and material removal rate (with or without fillers). In addition, pressure and traverse speed were (approximately equal) most effective factors for kerf inclination (with or without fillers). When the cutting surfaces were examined by electron microscopy, fiber delamination and pullouts were seen (Figure 14 (a)) in specimens without fillers material. Due to the absence of filler materials, this situation has been interpreted as the weakness of the matrix-fiber interface bond and the brittle behaviour of the matrix material. It has been observed (Figure 14 (b)) that the matrix-fiber interface bond on the cutting surface has improved with the addition of the filler materials.

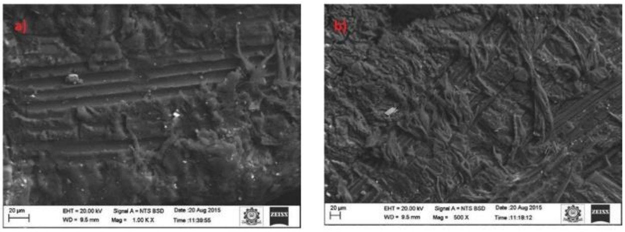

Figure 14. Material cutting surface: (a) without fillers material, (b) with fillers material (Jani et al., 2016)

Jagadish et al. (Jagadish, Bhowmik, & Ray, 2016) examined the effects of process parameters on surface roughness and cutting time in cutting sundi wood reinforced epoxy composite with AWJ. Box-Behnken experimental design and response surface methodology optimization design was used in the study. According to ANOVA analysis, significant process parameters for surface roughness were found as pressure, traverse speed and standoff distance, respectively. Also, traverse speed and standoff distance were significant process parameters for cutting time, respectively. Optimum cutting parameters values and corresponding response parameters values have been found with the response surface methodology and confirmation analysis were performed for verify the accuracy of the response surface methodology model. Prabu et al. (Prabu, Kumaran, & Uthayakumar, 2017) investigated the cutting of banana fiber reinforced polyester composite with AWJ. According to ANOVA analysis, standoff distance, pressure, traverse speed was found to be significant parameters for surface roughness, respectively. Also, the most significant parameter for the kerf angle was found standoff distance and then pressure. As a result, standoff distance was the most effective factor for both response parameters. Kumaran et al. (Kumaran, Ko, Uthayakumar, & Islam, 2017) examined the cutting of carbon fiber (two kinds-unidirectional (UD) and UD with a woven fabric surface) reinforced plastics with abrasive water jet. For surface roughness as response parameter, Taguchi experimental design was applied, and the results were evaluated by regression analysis. According to ANOVA analysis, important parameters have been found as pressure, standoff distance and traverse speed, respectively. When the contour plots of the surface roughness are examined, the values of high pressure and low traverse and standoff distance improved the surface roughness. Also, it has been stated that the UD with fabric surface specimens exhibited lower surface roughness. For surface roughness, Kumaran et al. (Kumaran, Ko, Kurniawan, Li, & Uthayakumar, 2017) examined the effect of experimental factors in cutting carbon fiber reinforced plastic composite with AWJ, then an adaptive neuro–fuzzy inference system (ANFIS) model has been developed by experimental results. According to ANOVA analysis, the most significant parameter was pressure and later standoff distance, and traverse speed were other significant parameters, respectively. In addition, optimum experimental condition was generated, then this material has been cut by AWJ. As a result, with the ANFIS model, predicted results were found at 95% confidence level and thus the suitability of the model created in experimental conditions was expressed. Muller et al. (Muller, D'Amato, & Rudawska, 2017) examined the cutting surface with SEM in cutting (microparticles of glass bead, corundum microparticles, short fibres of false banana Ensete Ventricosum and glass fabric/epoxy matrix) composite material with abrasive water jet. SEM images of the cutting surface of the material were shown in Figure 15. It has been stated that there was significant destruction in the composite layer with the penetration of the jet at the beginning of the cut surface. Thus, delamination and significant material removal were observed in this region. It was interpreted that the cut was regular at the continuation of the surface and delamination occurred according to the particle type. In addition, it was stated that the reinforcing (glass fabric, corundum and glass-bead particles) elements are cut from the matrix without delamination.

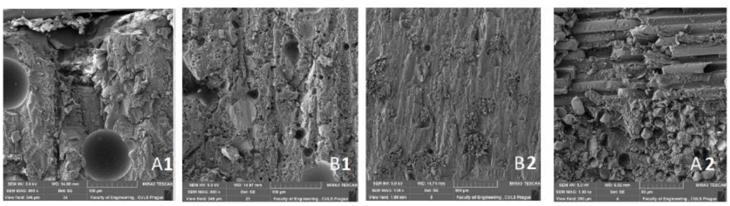

Figure 15. Fracture surface of the matrix with reinforcement-filler elements (a) microparticles of glass bead-matrix, (b) corundum microparticles-matrix, (c) short fibres of false banana Ensete Ventricosum-matrix, (d) glass fabric-matrix (Muller et al., 2017)

Kalirasu et al. (Kalirasu, Rajini, Rajesh, Jappes, & Karuppasamy, 2017) examined the cutting of jute polyester composite sheets produced in different thicknesses with AWJ. A hybrid function was created according to the surface roughness and kerf taper angle, and then Multi Objective Optimization by Ratio Analysis (MOORA) has been applied. Tests have been carried out according to the L27 experimental design. With the MOORA technique, the performance results were normalized and converted into dimensionless values using the related equation. Then optimum experimental parameters (same for both thicknesses) have been found according to the other applied procedures. The most effective parameter for surface roughness and kerf taper angle was traverse speed. Also, other effective parameters were standoff distance, pressure, respectively. It was stated that the prediction model created in low plate thickness was more compatible. In addition, predictive and experimental results were compared by other models. Different models were found to show differences in the formation of optimum experimental parameters. Popan et al. (Popan, Contiu, & Campbell, 2017) investigated the effect on the cutting surface of the standoff distance in cutting of carbon fiber reinforced epoxy composite with AWJ. According to the experimental study, when the standoff distance increased, the top kerf width and the top edge radius increased. In addition, as the standoff distance increased in the initial damage zone, the average surface roughness also increased. Armağan and Arici (Armağan & Arici, 2017) examined the cutting of glass fiber reinforced vinyl ester composite laminates (produced in various thickness) with AWJ. Taguchi experimental design constituted, and ANOVA analysis performed. In ANOVA analysis, standoff distance has been found as the most effective parameter for top kerf width, initial and zone average surface roughnesses response parameters. After optimum levels of experimental parameters for the response parameters were determined, confirmation tests realized. As a result, it was stated that the whole process was successfully carried out. Deepa et al. (Deepa, Padmanabhan, & Kuppan, 2017) processed the stack shaped composites (in Figure 16) as a test specimen.

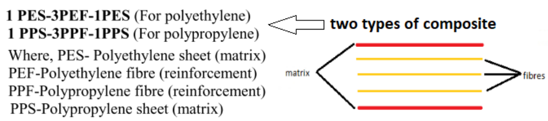

Figure 16. Forms of stack shaped composites (Deepa et al., 2017)

Selvam et al. (Selvam, Karunamoorthy, & Arunkumar, 2017) examined the cutting of glass-carbon/epoxy hybrid composite material with abrasive water jet. ANOVA analysis was done, and regression models were obtained with the response surface model (RSM). It was stated that traverse speed, pressure, abrasive flow rate were significant experimental parameters for kerf taper angle, also traverse speed was significant experimental parameter for surface roughness. The effects of binary test parameters level conditions on surface roughness and kerf taper angle were determined. Optimum cutting parameters levels have been determined according to RSM. As a result, the confirmation process was made with the estimated and experimental tests according to the optimum test parameters levels. Jagadeesh et al. (Jagadeesh, Dinesh Babu, Nalla Mohamed, & Marimuthu, 2018) investigated the cutting of carbon fiber reinforced epoxy composite laminates with AWJ. Box–Behnken design procedure and response surface method with variance analysis were used. Thus, the effects of test parameters on kerf taper angle and surface roughness were investigated. According to ANOVA analysis, traverse speed, standoff distance and standoff distance-traverse speed interaction were found to be significant for surface roughness. Also, according to ANOVA analysis, traverse speed, standoff distance and thickness were found significant for the kerf taper angle. The effects of binary test parameters level conditions on surface roughness and kerf taper angle were determined. For surface roughness and kerf taper angle, regression equations (mathematical models) were obtained with the response surface model (RSM). By making numerical optimization (with software) of experimental parameters, effects of parameters (for surface roughness and kerf taper angle) were determined. Finally, predicted and actual response values were compared using the best experimental parameters levels suggested by numerical optimization. Thus, it was stated that the model was valid. Murugan et al. (Murugan, Gebremariam, Hamedon, & Azhari, 2018) investigated the processing of polyoxymethylene with low pressure (at 34 MPa) abrasive water jet. As the traverse rate increased, the depth of penetration decreased. Popan et al. (Popan, Balc, Popan, & Carean, 2018) examined the effect of reverse engineering on the machining of carbon fiber reinforced epoxy composite with abrasive water jet. The process representation was shown in Figure 17. Master model and reverse engineering new part specimens have been cut in the same experimental conditions. As a result, the surface roughness values taken from various places was less in the master model specimen. Also, according to the dimensional measurements taken from various places in the specimens, dimensional accuracy deviation values have been lower in master model samples.

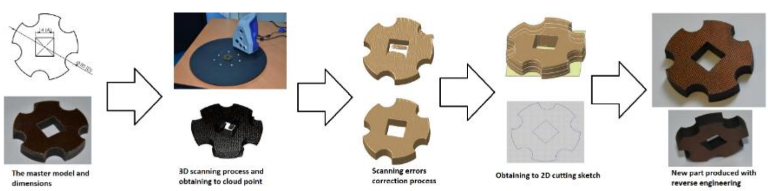

Figure 17. The process representation for study (Popan et al., 2018)

Ruiz-Garcia et al. (Ruiz-Garcia, Ares, Vazquez-Martinez, & Gómez, 2018) investigated the cutting of UNS A97050 stacks with AWJ. Both laminates for the stack have been provided in 5 mm thickness and the configurations of the stacks were aluminum alloy/CFRP and CFRP/aluminum alloy. Tests were carried out separately for the two configurations according to experimental design. SEM (Scanning Electron Microscopy)-SOM (Stereoscopic Optical Microscopy) images in cutting surface of the most aggressive experimental parameters were taken to see the delamination formation in CFRP. As shown in Figure 18, delamination was not observed in either configuration. In some test conditions, it was determined by SEM-SOM analysis that carbon particles were transported to aluminum alloy during processing. It was also stated that aluminum hasn't been found on carbon fiber.

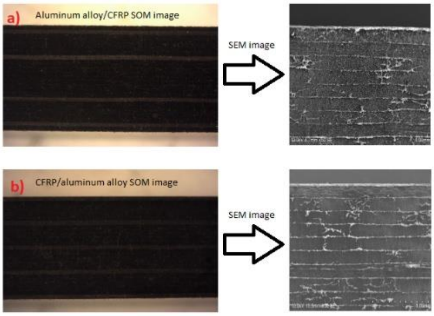

Figure 18. SOM and SEM images (a) aluminum alloy/CFRP, (b) CFRP/ aluminum alloy (Ruiz-Garcia et al., 2018)

Dhanawade and Kumar (Dhanawade & Kumar, 2018) investigated the effects of experimental parameters in cutting of carbon fiber reinforced epoxy composite material with AWJ. The cutting tests have been carried out according to the Taguchi experimental design (L16 orthogonal array). According to ANOVA analysis, the most significant parameter for surface roughness and kerf taper angle was pressure and then other significant parameter was traverse rate. As the pressure increases, surface roughness and kerf taper angle have decreased. However, as the traverse speed increased, surface roughness and kerf taper angle also increased. In the next stage of the study, the optimization of the experimental parameters was made with the grey relational analysis (GRA) approach. In the L16 experimental design, gray relation grades (GRG) values were found for each experiment. Figure 19 showed the GRG values intersection graph of the experimental parameters and levels for surface roughness and kerf taper angle. Here, the highest GRG values determined the optimum levels of the parameters. When ANOVA analysis of GRGs was performed, the pressure and traverse rate showed significant effects for surface roughness and kerf taper angle. The confirmation tests have been carried out according to the optimum parameters, surface roughness and kerf taper angle values were found less (based on experimental design results).

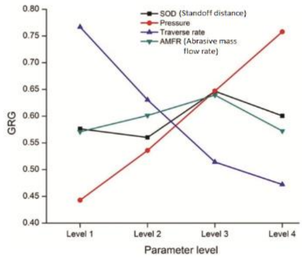

Figure 19. GRG values intersection graph of the experimental parameters and levels for surface roughness and kerf taper angle (Dhanawade & Kumar, 2018)

Jagadish et al. (Jagadish, Gupta, & Rajakumaran, 2018) investigated the cutting of pineapple filler based reinforced epoxy composite with AWJ. The effects of experimental parameters on material removal rate and surface roughness were determined according to the Taguchi test design. Thus, optimum levels of experimental parameters were found. Ramalingam et al. (Ramalingam, Bhaskar, Seshumadhav, & Allamraju, 2018) investigated the effects of experimental parameters on surface roughness and kerf taper angle in cutting of carbon fiber reinforced epoxy composite with abrasive water jet. AWJ cuts have been performed with the Taguchi experimental design (L27 orthogonal array). According to ANOVA analysis, the most significant parameter for surface roughness and kerf taper angle was mesh size. Other significant parameters for both surface roughness and kerf taper angle were abrasive mass flow rate and pressure, respectively. By Taguchi analysis, optimum levels of experimental parameters were found for surface roughness and kerf taper angle. Confirmation tests have been carried out for optimum conditions. For surface roughness and kerf taper angle, regression equations were created by response surface methodology. The results of the regression equations were found according to the optimum conditions and thus these values were compared with the confirmation test values. Müller et al. (Müller, Valášek, Linda, & Kolář, 2018) investigated the effects of the traverse speed on cutting of epoxy/micro particles from coconut shell composite material with AWJ/water jet (WJ). In both cutting methods (WJ/AWJ), traverse speed significantly affected the bottom kerf width. Through SEM images, it could be said that a better cutting surface was formed with abrasive water jet. Mm et al. (Mm, Azmi, Lee, & Mansor, 2018) investigated the cutting of carbon/glass fiber reinforced epoxy hybrid composite with abrasive water jet. The experimental plan was applied by a face-centered composite design. Moreover, the response parameters were kerf ratio and delamination factor. As seen in Figure 20, the delamination factor was found as the ratio of the maximum width of the delamination area to the actual cutting width. According to the normal probability plot and ANOVA analysis, significant parameters for kerf ratio were standoff distance and traverse rate, respectively. Then, according to the experimental results, an empirical model was developed using the response surface methodology. Delamination factor values were generally higher in the upper part of the kerf. When ANOVA analysis results were analyzed, significant parameters for the entrance delamination factor were abrasive flow rate, pressure, standoff distance (although p value was found to be insignificant, it was considered as p value was significant with the interaction of the traverse speed.), traverse rate and standoff distance-traverse rate interaction. In addition, significant parameters for the exit delamination factor were abrasive flow rate, pressure, traverse rate, abrasive flow rate-pressure interaction, abrasive flow rate-traverse rate interaction, pressure-traverse rate interaction. Thus, mathematical equations for entrance and exit delamination factors were created by experimental results. Optimum parameter levels have been determined by the response surface methodology for kerf ratio, entrance and exit delamination factors. Finally, optimization parameter levels were selected and then the predicted and experimental results were compared.

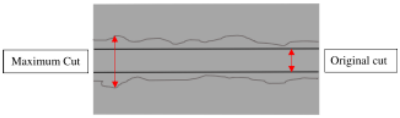

Figure 20. Finding the delamination factor (Mm et al., 2018)

El-Hofy et al. (El-Hofy et al., 2018) investigated the cutting of carbon fiber reinforced epoxy composites by AWJ. Two different lay-up composites were prepared for cutting and it has been determined as one of the test parameters. According to ANOVA analysis, standoff distance, traverse speed and pressure were significant parameters for top kerf width. Pressure, traverse speed and standoff distance parameters were found significant for bottom kerf width. In addition, it was stated that the pressure-traverse speed interaction was significant. Significant parameters of kerf taper were found as pressure and standoff distance. In addition, it was stated that the pressure-traverse speed interaction was significant. Main parameters have not been found significant for surface roughness. However, it was stated that the interactions between pressure-traverse speed, pressure-standoff distance, traverse speed-layup type and standoff distance-layup type were significant. Finally, an equation including processing cost calculation has been developed. Müller et al. (Müller, Valášek, & Kolář, 2018) investigated the cutting of hemp fibers or falsa banana (Ensete ventricosum) fibers or Jatropha Curcas L. microparticles reinforced epoxy composites at various traverse speeds with AWJ and WJ. Depending on the traverse speeds of the top and bottom kerf widths, the width values according to the cutting direction and jet type (AWJ or WJ) were given graphically. In addition, the results for the taper angle were given as a table. Ming et al. (Ming Ming, Azmi, Chuan, & Mansor, 2018) examined the effects of test parameters on the surface roughness in cutting of carbon/glass fiber reinforced epoxy hybrid composite with AWJ. An experimental plan has been created according to the face-centered composite design. Surface roughness values were taken from three zones (top, middle and bottom) of the cutting surface. Thus, the standard deviations of the values obtained from the zones were expressed graphically. The cutting surfaces of the specimens having the lowest and highest surface roughness values were examined with scanning electron microscope. Some defects (Figure 21) such as fiber pull out, debonding of the fiber-matrix interface, void, delamination have been detected on the cutting surfaces. The test results were most suitably defined by the quadratic polynomial models and ANOVA analysis was performed. According to this analysis, abrasive flow rate, pressure, standoff distance, traverse speed parameters and abrasive flow rate-pressure, abrasive flow rate-traverse speed, pressure-traverse speed interactions were significant. And then the model equation was generated for the roughness surface. It has been stated that optimum test parameters were found according to ANOVA analysis, response surface contour plots and perturbation plots. Finally, the optimum parameter levels were selected, and the experimental and predicted cutting results were compared.

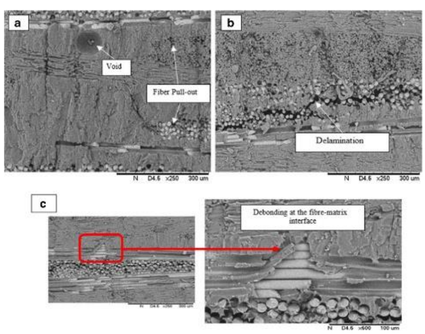

Figure 21. Some defects on the cutting surface (Ming Ming et al., 2018)

Kalirasu et al. (Kalirasu, Rajini, Rajesh, Siengchin, & Ramaswamy, 2018) examined the cutting of coconut sheath/unsaturated polyester (CS/UPR) composite with abrasive water jet. In the study, CS fiber was subjected to two different chemical (alkali (NaOH) and trichlorovinylsilane) treatments, thus chemical effects were examined. In the first stage, delamination was observed when the composite material exposed to chemical effect was cut with pure water jet. With reference to the previous study of the researchers, it was stated that the chemical treatment increased the crystallinity index, thereby it would increase the tensile strength of the fiber. The effects of the chemical treatments were shown in Figure 22 with SEM images. In Figure 22(a), chemical treatment was not made to the composite material. Here, a layer was seen which prevented the wettability of the fibers with the matrix. After the alkali chemical treatment, the said layer was removed, thereby the adhesion between the fiber with the matrix increased (Figure 22(b)). Silane formed a coating layer on the fiber surface (Figure 22(c). Thus, interfacial adhesion has occurred. Throughout the direction, the induced flexural strength due to AWJ machining has been examined. According to the graphs, the induced flexural strength decreased as various distances (radial distance of cutting front from free edge, vertical distance of cutting front towards depth) increased. The kerf taper angle values for traverse speed, standoff distance and pressure (varying experimental parameters) have been found as almost alkali chemical treatment (NTC)>without chemical treatment (UTC)>silan chemical treatment (STC). In addition, surface roughness values for traverse speed, standoff distance and pressure (varying experimental parameters) were interpreted as nearly NTC>STC>UTC.

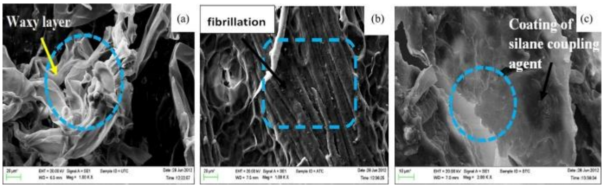

Figure 22. The effects of the chemical treatments (a) without chemical treatment, (b) alkali treated fiber, (c) silane treated fiber (Kalirasu et al., 2018)

Ares et al. (Ares, Mata, Ponce, & Gómez, 2019) investigated the effects of experimental parameters on kerf taper angle and surface roughness in cutting of carbon fiber reinforced epoxy composite with AWJ. Ra measurements on the cutting surface were taken from three different locations (zones) shown in Figure 23. Thus, the effects of experimental parameters on the cutting surface have been determined. According to ANOVA analysis, significant parameters for kerf taper angles were traverse speed and standoff distance. Then the significant parameters for zone 1 and zone 2 were traverse speed and standoff distance. In addition, significant parameters for zone 3 were found as traverse speed and abrasive mass flow rate. When the results were analyzed, traverse speed was found to be significant for each response parameter. The level effects of the parameters have been determined for the response results with the contour graphs between the significant parameters. Also, it was stated that the surface roughness decreased approximately 35 percent in the transition from zone 1 to zone 2.

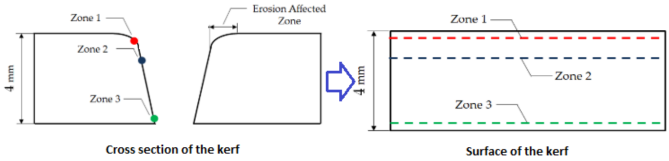

Figure 23. Measurements zones for surface roughness (Ares et al., 2019)

Pahuja et al. (Pahuja, Ramulu, & Hashish, 2019) investigated the cutting of stacked sheets with AWJ. The test parameters were selected as stacking configurations (Tİ/CFRP and CFRP/Ti), pressure and traverse speed. Figure 24 showed the test setup and measurement scheme, and it was noted that separation gap (1,6 mm) was added between Ti and CFRP. The *Ė/hu* function has been used to examine the effect of the change in jet energy on the surface roughness. Here, *Ė* was the jet energy, *h* was the penetration depth and *u* were the traverse speed. In the *Ė/hu* and surface roughness (R_a) interaction graph, two different regions were formed by a critical value. Despite the energy change in one region, the surface roughness value was stable while the other region has seen a rapid change. Since the critical value was higher in the CFRP/Ti configuration, it meant lower surface roughness was achieved at higher *Ė/hu*. According to the SEM examinations, it was stated that the fragmented abrasives or residuals left in the titanium layer adhered to the inlet side of the CFRP. When the interaction of kerf width with *Ė/hu* function was examined, (like surface roughness) a critical value and two regions were defined. Regression equations have been developed to estimate kerf width. The effects of experimental parameters levels on kerf widths and kerf angles were shown graphically with ANOVA analysis. In addition, percent contribution effects of experimental parameters were determined for kerf widths. Finally, a semi-analytical model was proposed to estimate to kerf width.

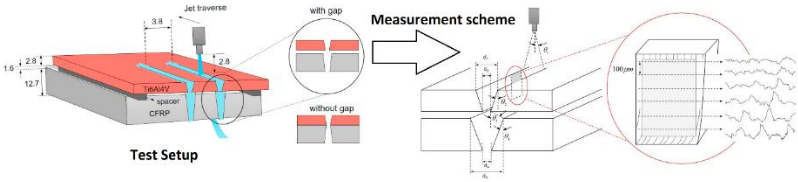

Figure 24. Test setup and measurement scheme (Pahuja et al., 2019)

Rao et al. (Rao, Mrudula, & Geethika, 2019) investigated the effects of experimental parameters on surface roughness (R_a), top kerf width (W_t) and material removal rate (MRR) in cutting of glass fiber reinforced epoxy composite (GFRP), carbon fiber reinforced epoxy composite (CFRP) and carbon-glass fibers reinforced epoxy hybrid composite (CGFRP) materials with AWJ. Experimental design was done with Taguchi L9 orthogonal arrays. According to these experiments, surface roughness values were generally found as CFRP> GFRP> CGFRP. In addition, the material removal rate values were found as CFRP> CGFRP> GFRP. Regression equations have been created for the response parameters of each three composites. Then three different multi-objective optimization problems (MOOPs) were defined for the equations. Thus, three models have been optimized with Non-dominated Sorting Genetic Algorithm (NSGA-II). Pareto optimal solutions were made for each material and the results including the three response parameters were shown with contour and surface plots. With the Single Best Compromise Pareto Solution, optimum cutting parameters have been found for the response parameters. Thus, confirmation tests were carried out with optimum cutting parameters. Jagadish et al. (Jagadish, Bhowmik, & Ray, 2019) investigated the effects of experimental parameters on surface roughness in cutting of sundi wood dust filled epoxy composite with abrasive water jet. The cuts were performed according to the Taguchi L27 experimental design, and then the optimum levels of experimental parameters have been found by Taguchi analysis. Cluster center information has been generated by the subtractive clustering (SC) method. Thus, a TSK-FL ((Takagi–Sugeno–Kang) - fuzzy logic) based model was used to estimate the surface roughness. Estimated surface roughness values were calculated according to the experimental design parameters and these results were compared with the experimental results. In addition, the significance of experimental parameters was determined according to experimental and estimated results with ANOVA analysis. Finally, various confirmation tests have been carried out. Xiao et al. (Xiao, Wang, Gao, & Soulat, 2019) investigated the effects of multi pass cutting and other experimental parameters on kerf taper and surface roughness in cutting of carbon fiber reinforced epoxy composite with AWJ. First, cutting surfaces were examined with SEM. Accordingly, defects such as pits were observed in the multi pass cutting. In addition, no delamination was observed in the single pass cutting and thus it was concluded that the multi pass cutting could be examined. In multi pass cutting, interlaminar delamination has been detected in the cutting surface exit zone. The material removal mechanism determined the occurrence of delamination. It was stated that delamination was affected by processing parameters levels and material properties. To compare the results, a control group was created in the experimental plan. This group included relatively low traverse speed and low-level pressure parameters. The low-pressure level and the angle of inclination effects reduced kerf taper value in multi pass cutting under constant test parameters. The advantage of inclination angle was eliminated at higher pressure level. In addition, kerf taper increased at high traverse speeds compared to single pass cutting (control group). In multi pass cutting under changed test parameters, kerf taper was reduced by choosing the first pass at the low-pressure level and the second pass at the higher-pressure level. Kerf taper value of single pass cutting was caught by designation of the appropriate test parameters. The utility of multi pass cutting to kerf taper and development of cutting time were shown graphically in Figure 25. Finally, under unchanged/changed test parameters in multi pass cutting, parameter levels where surface roughness has improved (according to control group) have been found.

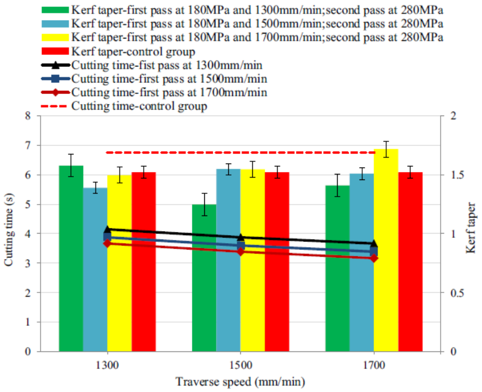

Figure 25. The utility of multi pass cutting to kerf taper and development of cutting time (Xiao et al., 2019)

Conclusion

Abrasive Water Jet (AWJ) machining has proven to be a highly effective technique for processing polymer and polymer matrix composites. Its ability to handle complex geometries while minimizing heat-affected zones and tool wear makes it a preferred choice over traditional methods. The literature reveals that AWJ performance is significantly influenced by parameters such as water pressure, abrasive type and flow rate, traverse speed, and standoff distance. Optimizing these parameters enhances surface finish, reduces delamination, and improves cutting precision.

Furthermore, advancements in nozzle design, the incorporation of oscillation techniques, and the introduction of polymer additives into the cutting stream have shown promising improvements in cut quality. Future research should focus on refining predictive models for cutting depth and surface quality, exploring environmentally friendly abrasives, and enhancing automation to ensure process repeatability and efficiency.

In conclusion, AWJ machining stands out as a versatile and sustainable solution for machining polymers and their composites. Continued investigation into process optimization and innovative techniques will further unlock its potential in manufacturing industries, driving improvements in productivity and product quality.

Table 1. General factors of the studies for AWJ cutting

Author	Target Material / Workpiece	Abrasive Material	Variable Process Parameters	Studies	Response
M. Hashish (Mohamed, 1988)	Polymethylmethacrylate Polycarbonate	Unknown	Traverse speed, Particle size, cutting angle, Abrasive flow rate, Hole drilling, Plain waterjet, Multipass cutting, Through cutting	Visualization of various stages, Entry length after which jet reaches maximum depth, Depth of cut, Penetration rate, Initial angle of jet-solid interface	
M. Ramulu, D. Arola (Ramulu & D.AROLA, 1992)	Unidirectional graphite/epoxy composite	Garnet	Fibre orientatiton,	Surface roughness, SEM observations,	
M. Hashish et al. (M. Hashish et al., 1997)	Printed circuit board, Graphite epoxy, (SUPER-WATER®) polymer additive in AWJ water	Garnet	Pressure, Traverse rate, (SUPER-WATER®) polymer additive in AWJ water,	Depth of cut, Traverse rate	
J. Wang (Jun Wang, 1999)	Teflon fabric/phenolic resin composite	Garnet	Pressure, Traverse speed, Standoff distance	Kerf width, Kerf taper angle, Surface roughness	
J. Wang, D.M. Guo (J. Wang & Guo, 2002)	Phenolic Fabric Polymer Matrix Composite	Garnet	Jet traverse rate, Abrasive flow rate, Water pressure	Depth of penetration	Predictive depth of penetration model
E. Lemma et al. (Lemma et al., 2002a)	Polymethylmethacrylate	Unknown	Oscillation angle, Frequency of oscillation, Traverse speed	Surface roughness	

E. Lemma et al. (Lemma et al., 2002b)	Glass fiber reinforced polymer composite	Unknown	Oscillation angle, Frequency of oscillation, Water-jet pressure, Abrasive mass flow rate, Nozzle traverse speed	Surface roughness	
F. L. Chen, E. Siores (Chen & Siores, 2003)	Polymethylmethac rylate	Garnet	Target material type	SEM observation s	
J. Wang et al. (J. Wang et al., 2003)	Phenolic fabric polymer matrix composite	Garnet	Water pressure, Traverse speed, Jet impact angle	Kerf width, Depth of penetration, Surface roughness	
R.T. Deam et al. (Deam et al., 2004)	Polymethylmethac rylate	Unknown	Traverse speed	Traces of the jet and solid interface, Intrinsic coordinate plot of cutting face, Cutting face curvature	Model produced, Comparison model with experimental data
E. Lemma et al. (Lemma et al., 2005)	Polymethylmethac rylate	Unknown	Pressure, Mass flow rate, Oscillation angle, Oscillation frequency, Traverse speed	Recorded images of the movement, Traces of the jet/solid interface	
M. Monno, C. Ravasio (Monno & Ravasio, 2005)	Rubber	Unknown	Standard equipment and splash-back damping equipment for fixing, Feed rate	Roughness, Vibration factors, Striation, Roughness index	Geometric model created and validation
C. Ma, R.T. Deam (Ma & Deam, 2006)	Acrylic	Garnet	Traverse speed, Standoff distance	Kerf width	Correlation for kerf width, Correlation coefficients for cutting speeds
H. Orbanic, M. Junkar (Orbanic & Junkar, 2008)	Polymethylmethac rylate	Garnet	Traverse speed	Inclination angle	Striation formation mechanism explanation
M.A. Azmir, A.K. Ahsan (Azmir & Ahsan, 2008)	Glass/epoxy composite	Garnet, Aluminium oxide	Form of fibre, Fibre volume fraction (%), Thickness of laminate, Abrasive types, Pressure, Standoff distance, Abrasive mass flow rate, Traverse rate, Cutting orientation	Surface roughness	Taguchi experimental design and ANOVA analysis, Confirmation test performed

D.K. Shanmugam et al. (Shanmugam et al., 2008)	Graphite (GY70-carbon fibres) / epoxy (type 934) resin composite	Garnet	Traverse speed, Water pressure, Delay time	Maximum crack length	Predictive delamination model conducted
M.A. Azmir, A.K. Ahsan (Azmir & Ahsan, 2009)	Glass fibre / epoxy composite	Garnet, Aluminium oxide	Pressure, Standoff distance, Abrasive flow rate, Traverse rate, Cutting orientation	Surface roughness, kerf taper ratio, SEM observation	Taguchi experimental design and ANOVA analysis
D.K. Shanmugam, S.H. Masood (Shanmugam & Masood, 2009)	Epoxy pre-impregnated graphite woven fabric (GY70 carbon, 934 epoxy) , glass / epoxy (781 glass, 5245C epoxy) composites		Traverse speed, Abrasive flow rate, Standoff distance, Water pressure	Kerf taper angle,	Predicted model and experimental data comparison
M.A. Azmir et al. (Azmir et al., 2009)	Aramid fibre (Kevlar 129) / phenolic resin composite	Garnet	Pressure, Abrasive mass flow rate, Standoff distance, Traverse rate	Surface roughness, Kerf taper ratio	Taguchi experimental design and ANOVA analysis, Linear regression analysis and predictive comparison
L.M. Hlaváć et al. (Hlaváč et al., 2009)	Plexiglass, Red plastic, yellow plastic	Garnet	Various target material	Limit traverse speed	Predicted and experimental traverse speeds for identified declination angle
T.U. Siddiqui, M. Shukla (Siddiqui & Shukla, 2010)	Kevlar-Epoxy Composite	Garnet	Water jet pressure, Traverse speed, Abrasive flow rate	Depth of cut,	Predicted depth of cut with mathematical model
Z. Zhenglong (Zou, 2012)	Carbon fiber/ glass fiber reinforced polymer composites	Natural corundum	Jet injection pressure, Cutting feed speed, Abrasive mass flow rate, Size of the grain	Depth of cut	Experimental analysis by ANOVA
A. Stoić et al. (Stoić et al., 2013)	Polyamide 6	Unknown	Cutting pressure, Cutting feed Abrasive mass flow	Surface roughness	
A. Alberdi et al. (Alberdi et al., 2013)	Carbon fiber reinforced polymer composite	Unknown	Various target material, Thickness, Percentage of traverse feed rate relative to the separation speed, Pressure, Abrasive mass flow rate, Standoff distance	Separation speed, Machinability index, Taper angle, Surface roughness	ANOVA analysis

P.F. Mayuet et al. (Mayuet et al., 2015)	Carbon fiber reinforced polymer composite	Garnet	Feed rate, Standoff distance, Abrasive flow rate	SEM and SOM observations	Delamination
R. Li et al. (R. Li et al., 2015)	Recombinant bamboo (Phenol formaldehyde resin addesive)	Unknown	Pressure, Feed Rate, Abrasive Mass Flow Rate, Thickness	Surface roughness	Box-Behnken design, Response surface methodology, ANOVA analysis, Regression equations, Confirmation test, Optimization
N. Ramesha et al. (Narayanappa Ramesha, 1 Siddaramaiah, 2016)	Banyan tree saw dust powder (BSD) filled Polypropylene (PP) green composites with/without maleic anhydride grafted PP (coupling agent) or talc (mineral filler)	Garnet	Pressure, Traverse speed, Filler effect, Coupling agent effect	Surface roughness, Kerf geometry by OPM, Kerf taper angle	
D.Hu et al. (Hu et al., 2016)	Marble target material, Polyacrylamide (PAM) additive in water of AWJ	Garnet	Standoff distance, Traverse rate, Additive	Kerf width, Surface roughness	
A. Dhanawade et al. (Dhanawade et al., 2016)	Carbon epoxy composite	Garnet	Standoff distance, Traverse rate, Jet pressure, Abrasive mass flow rate	Surface roughness, Kerf taper ratio, SEM observation	Taguchi experimental design, ANOVA analysis
S.P. Jani et et al. (Jani et al., 2016)	Kevlar/epoxy composite with/without palm shell and coconut shell fillers	Garnet	Water jet pressure, Traverse speed, Standoff distance, Abrasive flow rate	Kerf inclination, Material removal rate, Surface roughness, SEM observation	
Jagadish et al. (Jagadish et al., 2016)	Sundi wood/epoxy composite	Garnet	Pressure, Standoff distance, Traverse speed,	Surface roughness, Process time	Box-Behnken design (BBD) model, ANOVA analysis, Found of optimal parameters, Confirmation tests
V.A. Prabu et al. (Prabu et al., 2017)	Banana fiber reinforced polyester composite	Garnet	Water pressure, Traverse speed, Standoff distance	Surface roughness, Kerf angle,	ANOVA analysis,

				SEM observation	
S.T. Kumaran et al. (Kumaran, Ko, Kurniawan, et al., 2017)	Carbon fiber reinforced polymer composite	Garnet	Jet pressure, Traverse speed, Standoff distance	Surface roughness	Adaptive neuro–fuzzy inference system (ANFIS), ANOVA analysis, Confirmation tests
G. Barsukov et al. (Barsukov, Zhuravleva, & Kozhus, 2017)	Glass-cloth-based laminate	Garnet	Material thickness, pressure, Drifting, Lamination value of reference material at optimal technological mode	Lamination machinability index	Development of machinability criteria,
M. Muller et al. (Muller et al., 2017)	Microparticles of glass-bead B159- Corundum microparticles F80- Short fibres of false banana Ensete Ventricosum- Glass fabric/epoxy composite	Garnet	Filler/reinforcement material effect	SEM observation -EDX analysis	
S. Kalirasu et al. (Kalirasu et al., 2017)	Jute/polyester composite	Garnet	Pressure, Standoff distance, Feed rate	SEM observation, Surface roughness, Kerf taper angle	MOORA model, ANOVA analysis, Regression models,
S. T. Kumaran et al. (Kumaran, Ko, Uthayakumar, et al., 2017)	Carbon fiber reinforced polymer composite	Garnet	Jet pressure, Traverse rate, Standoff distance	Surface roughness	Taguchi orthogonal array, ANOVA analysis, Regression model
I.A. Popan et al. (Popan et al., 2017)	Carbon fiber/epoxy composite	Garnet	Standoff distance	Kerf width, Top edge radius, Surface roughness	Optical profilometer
M. Armağan, A.A. Arici (Armağan & Arici, 2017)	Glass fiber/vinyl ester composite	Garnet	Pressure, Abrasive mass flow rate, Traverse speed, Standoff distance, material thickness	Top Kerf width, Surface roughness	Taguchi design, ANOVA analysis, Optical profilometer, Regression analysis and confirmation test
A. Deepa et al.	Polyethylene matrix/reinforcement,	Unknown	Unknown	Tensile and Flexural test	

(Deepa et al., 2017)	Polypropylene matrix/reinforcement self-reinforced composites			properties, SEM observation	
R. Selvam et al. (Selvam et al., 2017)	Glass-Carbon/epoxy composite	Garnet	Traverse speed, Water pressure, Abrasive flow rate, Standoff distance	Kerf taper angle, Surface roughness	ANOVA analysis, Regression analysis, Response surface, Optimum values
B. Jagadeesh et al. (Jagadeesh et al., 2018)	Carbon/epoxy composite	Garnet	Standoff distance, Traverse rate, Thickness	Surface roughness, Kerf width, Kerf taper angle, SEM observation	Box–Behnken design, ANOVA analysis, Response surface method, Regression analysis, Optimization-Confirmation
M. Murugan et al. (Murugan et al., 2018)	Polyoxymethylene	Garnet	Traverse rate	Penetration depth, Kerf taper ratio, Surface roughness	
I.A. Popan (Popan et al., 2018)	Carbon/epoxy composite	Garnet	All conditions fixed	Surface roughness, Dimensional accuracy	Surface quality and Dimensional accuracy analysis
Ruiz-Garcia R. et al. (Ruiz-Garcia et al., 2018)	Carbon/epoxy composite and Aluminum alloy stack	Garnet	Water pressure, Traverse speed, Abrasive mass flow rate	SEM-SOM observations and EDS analysis, Kerf taper, Surface roughness	Straightness Deviation
A. Dhanawade, S. Kumar (Dhanawade & Kumar, 2018)	Carbon/epoxy composite	Garnet	Standoff distance, Jet pressure, Traverse rate, Abrasive mass flow rate	Surface roughness, Kerf taper angle, SEM observation	Taguchi design, ANOVA analysis, Grey relational analysis, Confirmation test
Jagadish et al. (Jagadish et al., 2018)	Pineapple filler/epoxy composite	Unknown	Standoff distance, Pressure, Traverse rate, Abrasive grain size	Material removal rate, Surface roughness	Taguchi design, Confirmation test
T. Ramalingam et al. (Ramalingam et al., 2018)	Carbon/epoxy composite	Garnet	Mesh size, Pressure, Abrasive mass flow rate, Standoff distance	Surface roughness, Kerf taper	Taguchi design, Regression equation, Confirmation test

M. Müller et al. (Müller, Valášek, Linda, et al., 2018)	Epoxy/microparticles from coconut shell composite	Garnet	Traverse speed	SEM observation, Kerf width	Also, water jet cutting realized
I.W. MM et al. (Mm et al., 2018)	Carbon-glass/epoxy composite	Garnet	Abrasive flow rate, Pressure, Standoff distance, Traverse rate	Kerf width, Kerf ratio, Delamination factor	ANOVA analysis, Response surface method, Optimization
M. El-Hofy et al. (El-Hofy et al., 2018)	Carbon/epoxy composite	Garnet ?	Pressure, Feed rate, Standoff distance, CFRP material type	Kerf width, Kerf taper, Surface roughness, Process cost	
M. Müller et al. (Müller, Valášek, & Kolář, 2018)	Fibres from hemp or false banana (Ensete ventricosum) or microparticles from Jatropha Curcas L. seedcakes/epoxy composite	Garnet	Traverse rate	Kerf width, Taper angle	
I.W.M. Ming et al. (Ming Ming et al., 2018)	Carbon/glass fiber reinforced composite	Garnet	Abrasive flow rate, Pressure, Standoff distance, Traverse rate	Surface roughness, SEM observation ,	Response surface methodology, ANOVA analysis
S. Kalirasu et al. (Kalirasu et al., 2018)	Coconut sheath/unsaturated polyester composite	Garnet	Alkali (NaOH) or trichlorovinylsilane chemical treatments for fiber, Traverse rate, Standoff distance, Pressure	SEM observation, Induced flexural strength, Kerf taper angle, Surface roughness	
P.F.M. Ares et al. (Ares et al., 2019)	Carbon/epoxy composite	Garnet	Traverse rate, Standoff distance, Abrasive mass flow rate	Taper angle, Surface roughness, SEM observation	ANOVA analysis
R. Pahuja et al. (Pahuja et al., 2019)	Ti6Al4V - Carbon/epoxy composite stack	Garnet	Pressure, Traverse speed, Stacking sequence	Surface roughness, SEM observation, Kerf width	ANOVA analysis, Regression model, Semi-analytical modeling
V.D.P. Rao et al. (Rao et al., 2019)	Carbon and/or glass fiber /composite	Unknown	Abrasive mass flow rate, Traverse rate, Standoff distance	Surface roughness, Kerf width, Material removal rate	Regression equations, Elitist Non-dominated Sorting Genetic Algorithm (MOOPs by NSGA-II are)

R. Pahuja, M. Ramulu (Pahuja & Ramulu, 2019)				Regression models developed using wavelet packets, predicted vs. observed Rz	Wavelet packet analysis of acoustic emission signals
Jagadish et al. (Jagadish et al., 2019)	Sundi wood dust / epoxy composite	Unknown	Abrasive grain size, Standoff distance, Pressure, Abrasive mass flow rate, Traverse rate	Surface roughness, Optimum process parameters,	Taguchi method, Fuzzy logic (FL), Takagi–Sugeno–Kang (TSK) fuzzy model with subtractive clustering (SC), TSK–FL model, ANOVA analysis, Confirmation test
S. Xiao et al. (Xiao et al., 2019)	Carbon/epoxy composite	Garnet	Pressure, Impact angles, Traverse speed, Single-multi pass cutting	SEM observation , Kerf taper, Cutting time, Surface roughness	
A. Sambruno et al. (Sambruno , Bañon, Salguero, Simonet, & Batista, 2019)	Carbon fiber/ polyurethane composite	Garnet	Pressure, Traverse rate, Abrasive mass flow rate	Kerf taper angle	Response surface methodology, ANOVA analysis, Mathematical model validation
M. Armağan, A.A. Arıcı (ARMAĞAN & ARICI, 2019)	Glass fiber/vinyl ester composite	Garnet	Nozzle slope angle	Surface roughness, SEM observation	
X. Li et al. (X. Li, Ruan, Zou, Long, & Chen, 2020)	Carbon fiber reinforced polymer composite	Garnet	Traverse speed, Abrasive mass flow rate, Water jet pressure, Standoff distance, Sample thickness	Surface roughness, Length of the smooth cutting region	Optical profilometer
K.R. Sumesh, K. Kanthavel (Sumesh K R, 2020)	Sisal/Pineapple epoxy hybrid and/or flyash filler from the waste of Bagasse (BGFA) - Banana (BFA) - Coir (CFA)	Garnet	Pressure, Combination of material (and untreated fiber), Standoff distance, Traverse speed	Material removal rate, SEM observation -EDX analysis, Surface roughness	

References

Ahmad, J. (2009). *Machining of Polymer Composites*. *Journal of Chemical Information and Modeling* (Vol. 53). Boston, MA: Springer US. Retrieved from https://doi.org/10.1007/978-0-387-68619-6

Alberdi, A., Suárez, A., Artaza, T., Escobar-Palafox, G. A., & Ridgway, K. (2013). Composite cutting with abrasive water jet. *Procedia Engineering*, 63(mm), 421–429. Retrieved from https://doi.org/10.1016/j.proeng.2013.08.217

Ares, P. F. M., Mata, F. G., Ponce, M. B., & Gómez, J. S. (2019). Defect analysis and detection of cutting regions in CFRP machining using AWJM. *Materials*, 12(24). Retrieved from https://doi.org/10.3390/ma1224055

Armağan, M., & Arici, A. A. (2017). Cutting performance of glass-vinyl ester composite by abrasive water jet. *Materials and Manufacturing Processes*, 32(15), 1715–1722. Retrieved from https://doi.org/10.1080/10426914.2016.1269919

ARMAĞAN, M., & ARICI, A. A. (2019). Aşındırıcılı Su Jetinde Eğimli Kesimin İncelenmesi. *Afyon Kocatepe Üniversitesi Fen Ve Mühendislik Bilimleri Dergisi*, 19(2), 480–489. Retrieved from https://doi.org/10.35414/akufemubid.552139

Arola, D., & Ramulu, M. (1997). Material removal in abrasive waterjet machining of metals a residual stress analysis. *Wear*, 211(2), 302–310. Retrieved from https://doi.org/10.1016/S0043-1648(97)00131-2

AWJ machine. (2020). Retrieved 10 March 2024, from https://www.omax.com/en/us/learn/how-does-waterjet-work

AWJ nozzle. (2020). Retrieved 11 March 2025, from https://www.omax.com/en/us/learn/how-does-waterjet-work

Azmir, M. A., & Ahsan, A. K. (2008). Investigation on glass/epoxy composite surfaces machined by abrasive water jet machining. *Journal of Materials Processing Technology*, 198(1–3), 122–128. Retrieved from https://doi.org/10.1016/j.jmatprotec.2007.07.014

Azmir, M. A., & Ahsan, A. K. (2009). A study of abrasive water jet machining process on glass/epoxy composite laminate. *Journal of Materials Processing Technology*, 209(20), 6168–6173. Retrieved from https://doi.org/10.1016/j.jmatprotec.2009.08.011

Azmir, M. A., Ahsan, A. K., & Rahmah, A. (2009). Effect of abrasive water jet machining parameters on aramid fibre reinforced plastics composite. *International Journal of Material Forming*, 2(1), 37–44. Retrieved from https://doi.org/10.1007/s12289-008-0388-2

Barsukov, G., Zhuravleva, T., & Kozhus, O. (2017). Quality of Hydroabrasive Waterjet Cutting Machinability. *Procedia Engineering*, 206, 1034–1038. Retrieved from https://doi.org/10.1016/j.proeng.2017.10.590

Cenna, A. A., & Mathew, P. (1997). Evaluation of cut quality of fibre-reinforced plastics - A review. *International Journal of Machine Tools and Manufacture*, 37(6), 723–736. Retrieved from https://doi.org/10.1016/S0890-6955(96)00085-5

Chen, F. L., & Siores, E. (2003). The effect of cutting jet variation on surface striation formation in abrasive water jet cutting. *Journal of Materials Processing Technology*, 135(1), 1–5. Retrieved from https://doi.org/10.1016/S0924-0136(01)00579-9

Deam, R. T., Lemma, E., & Ahmed, D. H. (2004). Modelling of the abrasive water jet cutting process. *Wear*, 257(9–10), 877–891. Retrieved from https://doi.org/10.1016/j.wear.2004.04.002

Deepa, A., Padmanabhan, K., & Kuppan, P. (2017). Machining and characterization of self-reinforced polymers. *IOP Conference Series: Materials Science and Engineering*, 263(6). Retrieved from https://doi.org/10.1088/1757-899X/263/6/062044

Dhanawade, A., & Kumar, S. (2018). Multi-performance optimization of abrasive water jet machining of carbon epoxy composite material. *Indian Journal of Engineering and Materials Sciences*, 25(5), 406–416.

Dhanawade, A., Kumar, S., & Kalmekar, R. V. (2016). Abrasive water jet machining of carbon epoxy composite. *Defence Science Journal*, 66(5), 522–528. Retrieved from https://doi.org/10.14429/dsj.66.9501

El-Hofy, M., Helmy, M. O., Escobar-Palafox, G., Kerrigan, K., Scaife, R., & El-Hofy, H. (2018). Abrasive Water Jet Machining of Multidirectional CFRP Laminates. *Procedia CIRP*, 68(April), 535–540. Retrieved from https://doi.org/10.1016/j.procir.2017.12.109

Hashish, M., Steele, D. E., & Bothell, D. H. (1997). Machining with super-pressure (690 MPa) waterjets. *International Journal of Machine Tools and Manufacture*, 37(4), 465–479. Retrieved from https://doi.org/10.1016/S0890-6955(96)00016-8

Hashish, Mohamed. (1984). A Modeling Study of Metal Cutting With Abrasive Waterjets. *Journal of Engineering Materials and Technology*, 106(1), 88–100. Retrieved from https://doi.org/10.1115/1.3225682

Hashish, Mohamed. (1989). An investigation of milling with abrasive-waterjets. *Journal of Manufacturing Science and Engineering, Transactions of the ASME*, 111(2), 158–166. Retrieved from https://doi.org/10.1115/1.3188745

Hashish, Mohamed. (1991). Characteristics of surfaces machined with abrasive-waterjets. *Journal of Engineering Materials and Technology, Transactions of the ASME*, 113(3), 354–362. Retrieved from https://doi.org/10.1115/1.2903418

Hlaváč, L. M., Hlaváčová, I. M., Gembalová, L., Kaličinský, J., Fabian, S., Měšťánek, J., … Mádr, V. (2009). Experimental method for the investigation of the abrasive water jet cutting quality. *Journal of Materials Processing Technology*, 209(20), 6190–6195. Retrieved from https://doi.org/10.1016/j.jmatprotec.2009.04.011

Hu, D., Tang, C. L., Kang, Y., & Li, X. (2016). An investigation on cutting quality by adding polymer in abrasive water jet. *Particulate Science and Technology*, 34(3), 352–358. Retrieved from https://doi.org/10.1080/02726351.2015.1082522

JACKSON C, & OLSON RD. (1969). *Shaped Tube Electrolytic Machining* (Vol. 69). Retrieved from https://doi.org/10.1361/asmhba0002158

Jagadeesh, B., Dinesh Babu, P., Nalla Mohamed, M., & Marimuthu, P. (2018). Experimental investigation and optimization of abrasive water jet cutting parameters for the improvement of cut quality in carbon fiber reinforced plastic laminates. *Journal of Industrial Textiles*, 48(1), 178–200. Retrieved from https://doi.org/10.1177/1528083717725911

Jagadish, Bhowmik, S., & Ray, A. (2016). Prediction and optimization of process parameters of green composites in AWJM process using response surface methodology. *International Journal of Advanced Manufacturing Technology*, 87(5–8), 1359–1370. Retrieved from https://doi.org/10.1007/s00170-015-8281-x

Jagadish, Bhowmik, S., & Ray, A. (2019). Prediction of surface roughness quality of green abrasive water jet machining: a soft computing approach. *Journal of Intelligent Manufacturing*, 30(8), 2965–2979. Retrieved from https://doi.org/10.1007/s10845-015-1169-7

Jagadish, Gupta, K., & Rajakumaran, M. (2018). Evaluation of machining performance of pineapple filler based reinforced polymer composites using abrasive water jet machining process. *IOP Conference Series: Materials Science and Engineering*, 430(1). Retrieved from https://doi.org/10.1088/1757-899X/430/1/012046

Jain, N. K., & Jain, V. K. (2001). Modeling of material removal in mechanical type advanced machining processes: A state-of-art review. *International Journal of Machine Tools and Manufacture*, 41(11), 1573–1635. Retrieved from https://doi.org/10.1016/S0890-6955(01)00010-4

Jani, S. P., Kumar, A. S., Khan, M. A., & Kumar, M. U. (2016). Machinablity of Hybrid Natural Fiber Composite with and without Filler as Reinforcement. *Materials and Manufacturing Processes*, 31(10), 1393–1399. Retrieved from https://doi.org/10.1080/10426914.2015.1117633

Kalirasu, S., Rajini, N., Rajesh, S., Jappes, J. T. W., & Karuppasamy, K. (2017). AWJM Performance of jute/polyester composite using MOORA and analytical models. *Materials and Manufacturing Processes*, 32(15), 1730–1739. Retrieved from https://doi.org/10.1080/10426914.2017.1279314

Kalirasu, S., Rajini, N., Rajesh, S., Siengchin, H. S., & Ramaswamy, S. N. (2018). AWJ machinability performance of CS/UPR composites with the effect of chemical treatment. *Materials and Manufacturing Processes*, 33(4), 452–461. Retrieved from https://doi.org/10.1080/10426914.2017.1328114

Kechagias, J., Petropoulos, G., & Vaxevanidis, N. (2012). Application of Taguchi design for quality characterization of abrasive water jet machining of TRIP sheet steels. *International Journal of Advanced Manufacturing Technology*, 62(5–8), 635–643. Retrieved from https://doi.org/10.1007/s00170-011-3815-3

Komanduri, R. (1997). Machining of fiber-reinforced composites. *Machining Science and Technology*, 1(1), 113–152. Retrieved from https://doi.org/10.1080/10940349708945641

Kumaran, S. T., Ko, T. J., Kurniawan, R., Li, C., & Uthayakumar, M. (2017). ANFIS modeling of surface roughness in abrasive waterjet machining of carbon fiber reinforced plastics. *Journal of Mechanical Science and Technology*, 31(8), 3949–3954. Retrieved from https://doi.org/10.1007/s12206-017-0741-9

Kumaran, S. T., Ko, T. J., Uthayakumar, M., & Islam, M. M. (2017). Prediction of surface roughness in abrasive water jet machining of CFRP composites using regression analysis. *Journal of Alloys and Compounds*, 724, 1037–1045. Retrieved from https://doi.org/10.1016/j.jallcom.2017.07.108

Lemma, E., Chen, L., Siores, E., & Wang, J. (2002a). Optimising the AWJ cutting process of ductile materials using nozzle oscillation technique. *International Journal of Machine Tools and Manufacture*, 42(7), 781–789. Retrieved from https://doi.org/10.1016/S0890-6955(02)00017-2

Lemma, E., Chen, L., Siores, E., & Wang, J. (2002b). Study of cutting fiber-reinforced composites by using abrasive water-jet with cutting head oscillation. *Composite Structures*, 57(1–4), 297–303. Retrieved from https://doi.org/10.1016/S0263-8223(02)00097-1

Lemma, E., Deam, R., & Chen, L. (2005). Maximum depth of cut and mechanics of erosion in AWJ oscillation cutting of ductile materials. *Journal of Materials*

Processing Technology, 160(2), 188–197. Retrieved from https://doi.org/10.1016/j.jmatprotec.2004.06.010

Li, R., Ekevad, M., Guo, X., Cao, P., Wang, J., Chen, Q., & Xue, H. (2015). Pressure, feed rate, and abrasive mass flow rate influence on surface roughness for recombinant bamboo abrasive water jet cutting. *BioResources*, 10(2), 1998–2008. Retrieved from https://doi.org/10.15376/biores.10.2.1998-2008

Li, X., Ruan, X., Zou, J., Long, X., & Chen, Z. (2020). Experiment on carbon fiber–reinforced plastic cutting by abrasive waterjet with specific emphasis on surface morphology. *International Journal of Advanced Manufacturing Technology*, 107(1–2), 145–156. Retrieved from https://doi.org/10.1007/s00170-020-05053-y

Ma, C., & Deam, R. T. (2006). A correlation for predicting the kerf profile from abrasive water jet cutting. *Experimental Thermal and Fluid Science*, 30(4), 337–343. Retrieved from https://doi.org/10.1016/j.expthermflusci.2005.08.003

Mayuet, P. F., Girot, F., Lamíkiz, A., Fernández-Vidal, S. R., Salguero, J., & Marcos, M. (2015). SOM/SEM based Characterization of Internal Delaminations of CFRP Samples Machined by AWJM. *Procedia Engineering*, 132, 693–700. Retrieved from https://doi.org/10.1016/j.proeng.2015.12.549

Ming Ming, I. W., Azmi, A. I., Chuan, L. C., & Mansor, A. F. (2018). Experimental study and empirical analyses of abrasive waterjet machining for hybrid carbon/glass fiber-reinforced composites for improved surface quality. *International Journal of Advanced Manufacturing Technology*, 95(9–12), 3809–3822. Retrieved from https://doi.org/10.1007/s00170-017-1465-9

Mm, I. W., Azmi, A., Lee, C., & Mansor, A. (2018). Kerf taper and delamination damage minimization of FRP hybrid composites under abrasive water-jet machining. *International Journal of Advanced Manufacturing Technology*, 94(5–8), 1727–1744. Retrieved from https://doi.org/10.1007/s00170-016-9669-y

Mohamed, H. (1988). Visualization of the abrasive-waterjet cutting process. *Experimental Mechanics*, 28.2, 159–169.

Monno, M., & Ravasio, C. (2005). The effect of cutting head vibrations on the surfaces generated by waterjet cutting. *International Journal of Machine Tools and Manufacture*, 45(3), 355–363. Retrieved from https://doi.org/10.1016/j.ijmachtools.2004.07.010

Muller, M., D'Amato, R., & Rudawska, A. (2017). Machining of polymeric composites by means of abrasive water-jet technology. *Engineering for Rural Development*, 16, 121–127. Retrieved from https://doi.org/10.22616/ERDev2017.16.N021

Müller, M., Valášek, P., & Kolář, V. (2018). Research on application of technology using water jet on machining of polymeric composite biological-reinforced materials. *Manufacturing Technology*, 18(4), 630–634. Retrieved from https://doi.org/10.21062/ujep/152.2018/a/1213-2489/MT/18/4/630

Müller, M., Valášek, P., Linda, M., & Kolář, V. (2018). Research on water jet cutting of composites based on epoxy/microparticles from coconut shell. *MATEC Web of Conferences,* 244, 1–9. Retrieved from https://doi.org/10.1051/matecconf/201824402001

Murugan, M., Gebremariam, M., Hamedon, Z., & Azhari, A. (2018). Performance Analysis of Abrasive Waterjet Machining Process at Low Pressure. *IOP Conference Series: Materials Science and Engineering*, 319(1), 012051. Retrieved from https://doi.org/10.1088/1757-899X/319/1/012051

Narayanappa Ramesha, 1 Siddaramaiah, 2 Sania Akhtar. (2016). Abrasive Water Jet Machining and Mechanical Behavior of Banyan Tree Saw Dust Powder Loaded Polypropylene Green Composites. *Polymers and Polymer Composites*. Retrieved from https://doi.org/10.1002/pc

Orbanic, H., & Junkar, M. (2008). Analysis of striation formation mechanism in abrasive water jet cutting. *Wear*, 265(5–6), 821–830. Retrieved from https://doi.org/10.1016/j.wear.2008.01.018

Pahuja, R., & Ramulu, M. (2019). Surface quality monitoring in abrasive water jet machining of Ti6Al4V–CFRP stacks through wavelet packet analysis of acoustic emission signals. *International Journal of Advanced Manufacturing Technology*, 104(9–12), 4091–4104. Retrieved from https://doi.org/10.1007/s00170-019-04177-0

Pahuja, R., Ramulu, M., & Hashish, M. (2019). Surface quality and kerf width prediction in abrasive water jet machining of metal-composite stacks. *Composites Part B: Engineering*, 175(July), 107134. Retrieved from https://doi.org/10.1016/j.compositesb.2019.107134

Popan, I. A., Balc, N., Popan, A., & Carean, A. (2018). Experimental study on reverse engineering in case of composite materials cut by water jet cutting. *MATEC Web of Conferences,* 178, 4–9. Retrieved from https://doi.org/10.1051/matecconf/201817803004

Popan, I. A., Contiu, G., & Campbell, I. (2017). Investigation on standoff distance influence on kerf characteristics in abrasive water jet cutting of composite materials. *MATEC Web of Conferences*, 137. Retrieved from https://doi.org/10.1051/matecconf/201713701009

Prabu, V. A., Kumaran, S. T., & Uthayakumar, M. (2017). Performance Evaluation of Abrasive Water Jet Machining on Banana Fiber Reinforced Polyester

Composite. *Journal of Natural Fibers*, 14(3), 450–457. Retrieved from https://doi.org/10.1080/15440478.2016.1212768

Ramalingam, T., Bhaskar, S., Seshumadhav, K., & Allamraju, K. V. (2018). Optimization of process parameters in bi-directional carbon fiber composite using AWJM. *Materials Today: Proceedings*, 5(9), 18933–18940. Retrieved from https://doi.org/10.1016/j.matpr.2018.06.243

Ramulu, M., & D.AROLA. (1992). Water Jet and abrasive water jet cutting of unidirectional graphite/epoxy composites.

Rao, V. D. P., Mrudula, M., & Geethika, V. N. (2019). Multi-objective Optimization of Parameters in Abrasive Water Jet Machining of Carbon-Glass Fibre-Reinforced Hybrid Composites. *Journal of The Institution of Engineers (India): Series D*, 100(1), 55–66. Retrieved from https://doi.org/10.1007/s40033-019-00181-6

Ruiz-Garcia, R., Ares, P. F. M., Vazquez-Martinez, J. M., & Gómez, J. S. (2018). Influence of abrasive waterjet parameters on the cutting and drilling of CFRP/UNS A97075 and UNS A97075/CFRP stacks. *Materials*, 12(1). Retrieved from https://doi.org/10.3390/ma12010107

Sambruno, A., Bañon, F., Salguero, J., Simonet, B., & Batista, M. (2019). Kerf Taper Defect Minimization Based on Abrasive Waterjet Machining of Low Thickness Thermoplastic Carbon Fiber Composites C/TPU. *Materials*, 12(24), 4192. Retrieved from https://doi.org/10.3390/ma12244192

Selvam, R., Karunamoorthy, L., & Arunkumar, N. (2017). Investigation on performance of abrasive water jet in machining hybrid composites. *Materials and Manufacturing Processes*, 32(6), 700–706. Retrieved from https://doi.org/10.1080/10426914.2016.1198039

Shanmugam, D. K., & Masood, S. H. (2009). An investigation on kerf characteristics in abrasive waterjet cutting of layered composites. *Journal of Materials Processing Technology*, 209(8), 3887–3893. Retrieved from https://doi.org/10.1016/j.jmatprotec.2008.09.001

Shanmugam, D. K., Nguyen, T., & Wang, J. (2008). A study of delamination on graphite/epoxy composites in abrasive waterjet machining. *Composites Part A: Applied Science and Manufacturing*, 39(6), 923–929. Retrieved from https://doi.org/10.1016/j.compositesa.2008.04.001

Siddiqui, T. U., & Shukla, M. (2010). Modeling of depth of cut in abrasive waterjet cutting of thick Kevlar-epoxy composites. *Key Engineering Materials*, 443, 423–427. Retrieved from https://doi.org/10.4028/www.scientific.net/KEM.443.423

Stoić, A., Duspara, M., Kosec, B., Stoić, M., & Samardžić, I. (2013). Application of water jet for cutting polymer materials. *Metalurgija*, 52(2), 255–258.

Sumesh K R, K. K. (2020). Abrasive water jet machining of Sisal/Pineapple epoxy hybrid composites with the addition of various fly ash filler. *Materials Research Express*. Retrieved from https://doi.org/10.1088/2053-1591/ab7865

Sureban, R., Kulkarni, V. N., & Gaitonde, V. N. (2019). Modern optimization techniques for advanced machining processes - A review. *Materials Today: Proceedings*, 18, 3034–3042. Retrieved from https://doi.org/10.1016/j.matpr.2019.07.175

Temuçin, T., Tozan, H., Vayvay, Ö., Harničárová, M., & Valíček, J. (2014). A fuzzy based decision model for nontraditional machining process selection. *International Journal of Advanced Manufacturing Technology*, 70(9–12), 2275–2282. Retrieved from https://doi.org/10.1007/s00170-013-5474-z

Wang, J., & Guo, D. M. (2002). A predictive depth of penetration model for abrasive waterjet cutting of polymer matrix composites. *Journal of Materials Processing Technology*, 121(2–3), 390–394. Retrieved from https://doi.org/10.1016/S0924-0136(01)01246-8

Wang, J., Kuriyagawa, T., & Huang, C. Z. (2003). An experimental study to enhance the cutting performance in abrasive waterjet machining. *Machining Science and Technology*, 7(2), 191–207. Retrieved from https://doi.org/10.1081/MST-120022777

Wang, Jun. (1999). Machinability study of polymer matrix composites using abrasive waterjet cutting technology. *Journal of Materials Processing Technology*, 94(1), 30–35. Retrieved from https://doi.org/10.1016/S0924-0136(98)00443-9

Xiao, S., Wang, P., Gao, H., & Soulat, D. (2019). A study of abrasive waterjet multi-pass cutting on kerf quality of carbon fiber-reinforced plastics. *International Journal of Advanced Manufacturing Technology*, 105(11), 4527–4537. Retrieved from https://doi.org/10.1007/s00170-018-3177-1

Yao, Y. L., Cheng, G. J., Rajurkar, K. P., Kovacevic, R., Feiner, S., & Zhang, W. (2005). Combined research and curriculum development of nontraditional manufacturing. *International Journal of Phytoremediation*, 30(3), 363–376. Retrieved from https://doi.org/10.1080/03043790500114581

Zou, Z. (2012). Study of cutting composite materials with low pressure abrasive-water jet. *Applied Mechanics and Materials*, 130–134, 1480–1483. Retrieved from https://doi.org/10.4028/www.scientific.net/AMM.130-134.1480